

Recursive Estimation for Sparse Gaussian Process Regression

Manuel Schürch^{1,2}, Dario Azzimonti¹, Alessio Benavoli^{3,1}, and Marco Zaffalon¹

¹*Istituto Dalle Molle di Studi sull'Intelligenza Artificiale (IDSIA); Manno, Switzerland*

²*Università della Svizzera italiana (USI); Lugano, Switzerland*

³*University of Limerick (UL); Limerick, Ireland*

May 29, 2019

Abstract

Gaussian Processes (GPs) are powerful kernelized methods for non-parametric regression used in many applications. However, their plain usage is limited to a few thousand of training samples due to their cubic time complexity. In order to scale GPs to larger datasets, several sparse approximations based on so-called inducing points have been proposed in the literature. The majority of previous work has focused on the batch setting, whereas in this work we focusing on the training with mini-batches. In particular, we investigate the connection between a general class of sparse inducing point GP regression methods and Bayesian recursive estimation which enables Kalman Filter and Information Filter like updating for online learning. Moreover, exploiting ideas from distributed estimation, we show how our approach can be distributed. For unknown parameters, we propose a novel approach that relies on recursively propagating the analytical gradients of the posterior over mini-batches of the data. Compared to state of the art methods, we have analytic updates for the mean and covariance of the posterior, thus reducing drastically the size of the optimization problem. We show that our method achieves faster convergence and superior performance compared to state of the art sequential Gaussian Process regression on synthetic GP as well as real-world data with up to a million of data samples.

Keywords: Gaussian processes; Recursive estimation; Kalman filters; Non-parametric regression; Parameter estimation.

1 Introduction

Regression methods based on *Gaussian processes* (GPs) are used in many machine learning applications due to their modelling flexibility, robustness to overfitting and availability of well-calibrated predictive uncertainty estimates. The areas of applications range from social and natural science through engineering. In the area of control engineering, GPs have been used in system identification for impulse response estimation [24, 7, 25, 23], nonlinear ARX models [17, 3], learning of ODEs [1, 19] and latent force modelling [37]. The problem of learning the state space of a nonlinear dynamical system using GPs is discussed in [9, 21, 33]. Besides the many benefits, GPs have one main drawback: they are not suitable for large data sets due to their $\mathcal{O}(N^2)$ memory requirements and $\mathcal{O}(N^3)$ computational cost, where N is the number of training samples.

Over the past decade, many different approximations were developed to reduce this cost. The most common and successful methodology to approximate GPs is based on so-called *inducing point* methods, where the unknown function is represented by its values at a set of M pseudo-inputs (called inducing points), with $M \ll N$. Early attempts to sparse GP regression were based on the *Subset of Regressors* (SoR/DIC) approximation due to [30, 36, 31]. However, these methods produce overconfident predictions when leaving the training data. In order to produce sensible uncertainty estimates, *Deterministic Training Conditional* (DTC) [8, 29], *Fully Independent Training Conditional* (FITC)

[32], *Fully Independent Conditional* (FIC) [26] and *Partially Independent Training Conditional* (PITC) [26] were suggested where in each model the joint prior over the latent function and test values is modified differently. Titsias [34] instead proposed to retain the exact prior but to perform approximate (variational) inference, leading to the *Variational Free Energy* (VFE) method which converges to full GP as M increases. Based on the minimization of an α -divergence, Bui et al. [5] presented *Power Expectation Propagation* (PEP), which unifies several of the previous mentioned models. Inference in such models can typically be done in $\mathcal{O}(M^2N)$ time and $\mathcal{O}(MN)$ space. In order to find good parameters (inducing input points and kernel hyperparameters), either the marginal log-likelihood of the sparse models or a lower bound are used as an objective function for numerical optimization.

The majority of previous work in GP approximation has focused on the batch setting, that is, all data is available at once and can be processed together. However, for big data, where the number of samples N can be many millions, keeping all data in memory is not possible and the data might even arrive sequentially.

In a streaming setup, Bui et al. [4] developed an algorithm to update hyperparameters in an online fashion. While this method is promising in this setting, its accuracy is limited by considering each sample only once. In this work we focus on the common setting where hyperparameters are learned by reconsidering mini-batches several times. In order to speed up the optimization, we would like to update the parameters more frequently for a subset of data and update the posterior in a sequential way.

In this setting, Hensman et al. [12] applied *Stochastic Variational Inference* (SVI, [14]) to an *uncollapsed* lower bound of the marginal likelihood. Compared to the *collapsed* bound of the VFE model, the (variational) posterior distribution is not eliminated analytically and is an explicit part of the objective function. The resulting *Stochastic Variational Gaussian Process* (SVGP) method allows to optimize the parameters with mini-batches of the data. One limitation of SVGP is the large number of parameters ($\approx MD + M^2$, where D is the input space dimension) to be numerically estimated since the update of the posterior distribution is not given analytically which leads to a high dimensional optimization problem.

Inspired by the work of [12], the authors in [22] demonstrated the high scalability of this method by exploiting distributed machine learning platforms. The

work of [12] was extended by [13] to the DTC, FI(T)C and PITC models for a variational anytime framework based on SVI with the corresponding uncollapsed bounds. However, it was assumed that the parameters are given in advance, that is, only the (variational) posterior distribution is learnt via SVI.

Although showing high scalability and desirable approximation, all these methods based on SVI have two main drawbacks: i) the (variational) posterior is not given analytically, which leads to $\mathcal{O}(M^2)$ additional many parameters; ii) the uncollapsed bounds are in practice often less tight than the corresponding collapsed batch bounds because the (variational) posterior is not optimally eliminated. Overall, the huge number of parameters leads to an optimization problem that is hard to tune and relies particularly on appropriately decaying learning rates. Even for fixed parameters, when no non-linearity is involved, there is still the need of reconsidering each sample many times.

An orthogonal direction was pursued by the authors in [11] and [28], where a connection between GPs and State Space models for particular kernels was established for spatio-temporal regression problems, which allows to apply sequential algorithm such as the Kalman Filter, see also [6, 2]. Inspired by this line of research, the authors in [35] focused on efficient implementation and extended the methodology to varying sampling locations over time. Although these approaches can deal with sequential data and solve the problem of temporal time complexity, the space complexity is still cubic in the number of measurements. In addition, the hyperparameters are assumed to be fixed in advance.

In order to improve these shortcomings, we show that sparse inducing point models can be seen as a Bayesian kernelized linear regression model with input dependent observation noise with a particular choice of basis and noise covariance function, respectively. Given these insights, we show how to apply recursive estimation algorithms like the Kalman Filter (KF) and Information Filter (IF) [15], which allows to train sparse GP methods analytically and exactly in an online or distributed setting (considering each sample only once, as opposed to the work in [12] and [13]) for given parameters. After processing all data, the obtained posterior distribution is equivalent to the corresponding batch version. This might constitute an interesting method on its own for many applications where there is prior knowledge about the parameters or they can be

estimated offline.

For unknown parameters, we propose a *recursive collapsed* lower bound to the marginal log likelihood, which can be used for stochastic optimization with mini-batches. Our approach is based on recursively exploiting the chain rule for derivatives by recursively propagating the analytical gradients of the posterior which enables to compute the derivatives of the lower bound sequentially. When computing the gradients of the recursive collapsed bound in a non-stochastic way, they exactly match the corresponding batch ones. This approach constitutes an efficient method to train a very general class of sparse GP regression models with much fewer parameters to be estimated numerically ($\approx MD$) than state of the art sequential GP regression methods ($\approx MD + M^2$). Since the number M of inducing points determines the quality of the approximation to full GP, this reduction in number of parameters from M^2 to M is crucial and results in more accurate and faster convergence than the state of the art approach (SVGP), which we demonstrate in several experiments.

In Section 2, we briefly review exact and sparse GP for regression in the batch case as well as the state of the art for sequential sparse GP learning. In Section 3, we establish the connection between sparse GP regression and recursive estimation by introducing a Bayesian kernelized linear regression model with input dependent observation noise for which we discuss the batch as well as its recursive solutions for given parameters. For unknown parameters, we propose in Section 4 a novel learning procedure - *Stochastic Recursive Gradient Propagation* (SRGP)¹ - based on recursively propagating the analytic gradients of the posterior, which allows to optimize the parameters with mini-batches. We demonstrate in Section 5 the resulting faster convergence and the superior performance of our proposed algorithm for synthetic as well real-world data with up to a million of samples. Section 6 concludes the work and presents future research directions.

2 GP Regression

Suppose we are given a training set $\mathcal{D} = \{y_i, \mathbf{x}_i\}_{i=1}^N$ of N pairs of inputs $\mathbf{x}_i \in \mathbb{R}^D$ and noisy scalar outputs y_i generated by adding independent Gaussian noise to a latent function $f(\mathbf{x})$, that is $y_i = f(\mathbf{x}_i) + \varepsilon_i$, where $\varepsilon_i \sim$

¹Code is available on <https://github.com/manuelIDSIA/SRGP>.

$\mathcal{N}(0, \sigma_n^2)$. We denote with $\mathbf{y} = [y_1, \dots, y_N]^T$ the vector of observations and with $\mathbf{X} = [\mathbf{x}_1^T, \dots, \mathbf{x}_N^T]^T \in \mathbb{R}^{N \times D}$.

We can model f with a *Gaussian Process* (GP), which defines a prior over functions and can be converted into a posterior over functions once we have observed some data (see e.g. [27]). To describe a GP, we only need to specify a mean $m(\mathbf{x})$ and a covariance function $k(\mathbf{x}, \mathbf{x}')$. The latter is a positive definite kernel function [27], for instance the *squared exponential* (SE) kernel with individual lengthscales for each dimension, that is $k(\mathbf{x}, \mathbf{x}') = \sigma_0^2 \exp\left(-\frac{1}{2}(\mathbf{x} - \mathbf{x}')^T \mathbf{L}^{-1}(\mathbf{x} - \mathbf{x}')\right)$

with $\mathbf{L} = \text{Diag}[l_1^2, \dots, l_D^2]$. We assume that the mean function is zero for the sake of simplicity and we use the SE kernel throughout this paper even though all methods introduced here work with any positive definite kernel. Since the joint prior $p(\mathbf{f}, f_*)$ on the training values $\mathbf{f} = f(\mathbf{X}) = [f(\mathbf{x}_1), \dots, f(\mathbf{x}_N)]^T$ and a test latent function value $f_* = f(\mathbf{x}_*)$ at an unknown test point $\mathbf{x}_* \in \mathbb{R}^D$ is multivariate Gaussian, it is straightforward to update this knowledge with observed data and thus doing inference analytically by manipulating multivariate Gaussian distributions. Combining it with the likelihood $p(\mathbf{y}|\mathbf{f}) = \mathcal{N}(\mathbf{y}|\mathbf{f}, \sigma_n^2 \mathbb{I})$ yields the posterior predictive distribution $p(f_*|\mathbf{y}) = \mathcal{N}(f_*|\boldsymbol{\mu}_*, \boldsymbol{\Sigma}_*)$ with

$$\begin{aligned} \boldsymbol{\mu}_* &= \mathbf{K}_{*X} (\mathbf{K}_{XX} + \sigma_n^2 \mathbb{I})^{-1} \mathbf{y} \\ \boldsymbol{\Sigma}_* &= \mathbf{K}_{**} - \mathbf{K}_{*X} (\mathbf{K}_{XX} + \sigma_n^2 \mathbb{I})^{-1} \mathbf{K}_{X*}. \end{aligned} \quad (1)$$

We define $[\mathbf{K}_{AB}]_{ij} = k(\mathbf{a}_i, \mathbf{b}_j)$ for any $\mathbf{A} \in \mathbb{R}^{M_1 \times D}$ and $\mathbf{B} \in \mathbb{R}^{M_2 \times D}$ with the corresponding rows $\mathbf{a}_i, \mathbf{b}_j$. For brevity, we use $*$ indicating \mathbf{x}_* . This posterior GP depends via the kernel matrices on the hyperparameters $\boldsymbol{\theta} = \{\sigma_0, l_1, \dots, l_D, \sigma_n\}$ which can be estimated by maximizing the log marginal likelihood

$$\log p(\mathbf{y}|\boldsymbol{\theta}) = \log \mathcal{N}(\mathbf{y}|\mathbf{0}, \mathbf{K}_{XX} + \sigma_n^2 \mathbb{I}). \quad (2)$$

Although this is an elegant approach for probabilistic regression, it is intractable for large datasets since the computations for inference require the inversion of the matrix in Eq. (1) which scales as $\mathcal{O}(N^3)$ in time and $\mathcal{O}(N^2)$ for memory (for given $\boldsymbol{\theta}$).

2.1 Batch Sparse GP Regression

In order to scale GPs to large data, several approaches have been proposed based on so-called *inducing point* methods, where the sparsity is achieved via $M \ll N$ inducing points $(\mathbf{u}, \mathbf{R}) \in (\mathbb{R}, \mathbb{R}^{M \times D})$ to optimally summarize the dependency of the whole training data. The

inducing *inputs* \mathbf{R} are in the D -dimensional input data space and the inducing *outputs* \mathbf{u} are the corresponding GP-function values $f(\mathbf{R})$ (consider also Figure 1). The GP prior over \mathbf{f} and f_* is augmented with the inducing outputs \mathbf{u} , leading to a joint $p(\mathbf{f}, f_*, \mathbf{u})$ and marginal $p(\mathbf{u}) = \mathcal{N}(\mathbf{0}, \mathbf{K}_{\mathbf{R}\mathbf{R}})$ prior, respectively. By marginalizing out the inducing points, the original prior $p(\mathbf{f}, f_*) = \int p(\mathbf{f}, f_* | \mathbf{u}) p(\mathbf{u}) d\mathbf{u}$ is recovered. The fundamental approximation in all sparse GP models is that given the inducing outputs \mathbf{u} , \mathbf{f} is independent for any f . Consequently, inference in these models can be done in $\mathcal{O}(M^2N)$ time and $\mathcal{O}(MN)$ space [32]. From an abstract point of view, inducing point methods differ from each other in 3 main aspects:

- I) **training**: inferring inducing outputs \mathbf{u} given inducing inputs \mathbf{R} and kernel hyperparameters θ
- II) **prediction**: performing prediction at a new test point \mathbf{x}_* given \mathbf{u} , \mathbf{R} and θ
- III) **optimization**: finding optimal inducing inputs \mathbf{R} and kernel hyperparameters θ

In the following, we briefly report a general sparse GP model due to [5] which unifies several previous sparse inducing point GP models in the batch case. It is based on the minimization of an α -divergence or can be equivalently seen as applying *Power Expectation Propagation* (PEP). We report the sparse predictive distribution which summarizes the training and prediction part as well as the bound to the marginal log-likelihood, which can be used for optimizing the parameters $\Theta = \{\theta, \mathbf{R}\}$. In the following, we denote $\mathbf{Q}_{AB} = \mathbf{K}_{AR} \mathbf{K}_{RR}^{-1} \mathbf{K}_{RB}$ and $\mathbf{D}_A = \mathbf{K}_{AA} - \mathbf{Q}_{AA}$ for any A, B . In the PEP model, the predictive distribution $p(f_* | \mathbf{y}) = \mathcal{N}(f_* | \boldsymbol{\mu}_*, \boldsymbol{\Sigma}_*)$ is given by

$$\begin{aligned} \boldsymbol{\mu}_* &= \mathbf{Q}_{*\mathbf{X}} (\overline{\mathbf{K}}_{\mathbf{X}\mathbf{X}} + \sigma_n^2 \mathbb{I})^{-1} \mathbf{y}, \\ \boldsymbol{\Sigma}_* &= \mathbf{K}_{**} - \mathbf{Q}_{*\mathbf{X}} (\overline{\mathbf{K}}_{\mathbf{X}\mathbf{X}} + \sigma_n^2 \mathbb{I})^{-1} \mathbf{Q}_{\mathbf{X}*}, \end{aligned} \quad (3)$$

where $\overline{\mathbf{K}}_{\mathbf{X}\mathbf{X}} = \mathbf{Q}_{\mathbf{X}\mathbf{X}} + \alpha \text{Diag}[\mathbf{D}_{\mathbf{X}}]$. For this model, a lower bound to the sparse log marginal likelihood is analytically available

$$\begin{aligned} \mathcal{L}_{PEP}(\Theta) &= \log \mathcal{N}(\mathbf{y} | \mathbf{0}, \overline{\mathbf{K}}_{\mathbf{X}\mathbf{X}} + \sigma_n^2 \mathbb{I}) \\ &\quad - \frac{1-\alpha}{2\alpha} \sum_{i=1}^N \log \left(1 + \frac{\alpha}{\sigma_n^2} [\mathbf{D}_{\mathbf{X}}]_{ii} \right), \end{aligned} \quad (4)$$

where we omit the explicit dependency on Θ via $\overline{\mathbf{K}}_{\mathbf{X}\mathbf{X}}$ and $\mathbf{D}_{\mathbf{X}}$ for the sake of brevity. Similar as with the

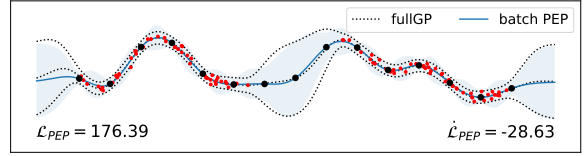


Figure 1: Full GP and batch sparse GP regression with PEP model ($\alpha = 0.5$). The $N = 100$ data samples are summarized with 15 inducing points (black dots), which are equidistantly placed. For illustration purposes, a slightly smaller than optimal lengthscale was selected and no parameters Θ were optimized. The numbers in the left and right corner indicate the lower bound to the marginal log likelihood in (4) and its derivative with respect to the lengthscale, respectively.

marginal likelihood (2) for full GP, this bound can be used to learn the parameters Θ . This model unifies several previous sparse GP inference approaches including FITC ($\alpha = 1$) [32] and VFE ($\alpha \rightarrow 0$) [34]. We want to highlight the special case $\alpha \rightarrow 0$, since it was the first approach where the approximating process was explicitly linked to full GP and it serves as starting point for the sequential case discussed below. Instead of modifying the prior and applying exact inference, the idea is to retain the exact prior and to perform approximate (variational) inference. In its original formulation, [34] proposed to maximize a variational lower bound to the true GP marginal likelihood, obtaining the *Variational Free Energy* (VFE) or the *collapsed lower bound*

$$\mathcal{L}_{VFE}(\Theta) = \log \mathcal{N}(\mathbf{y} | \mathbf{0}, \mathbf{Q}_{\mathbf{X}\mathbf{X}} + \sigma_n^2 \mathbb{I}) - \frac{\text{Tr}[\mathbf{D}_{\mathbf{X}}]}{2\sigma_n^2}, \quad (5)$$

where the variational distribution over the inducing points is optimally eliminated and analytically available. The novelty of this bound is that the rightmost term in (5) acts as a regularizer that prevents overfitting and has the effect that the sparse GP predictive distribution (3) converges rigorously [34] to the exact GP predictive distribution (1) for increasing number of inducing points when optimizing Θ with (5).

A more thorough overview of several sparse inducing point GP models is given in the Appendix B and for further details we refer to [5, 18, 26, 27] for recent reviews on the subject.

2.2 Sequential Sparse GP Regression

Focusing on the VFE model, the optimization for Θ of the collapsed lower bound (5) requires to process the whole dataset in a batch sense, which is very inefficient and not feasible for large N . We would like to update the parameters more frequently, therefore, we split the data $\mathcal{D} = \{\mathbf{y}_k, \mathbf{X}_k\}_{k=1}^K$ into K mini-batches of size B and denote \mathbf{f}_k the corresponding sparse GP value. In order to achieve faster convergence in the optimization, Hensman et al. [12] introduced *Stochastic Variational Gaussian Process* (SVGP) where they applied stochastic optimization to an *uncollapsed lower bound* to the log marginal likelihood

$$\begin{aligned} \mathcal{L}_{SVGP}(\boldsymbol{\mu}, \boldsymbol{\Sigma}, \Theta) = & -\text{KL}[q(\mathbf{u})||p(\mathbf{u}|\Theta)] \\ & + K \sum_{k=1}^K \int q(\mathbf{u}) p(\mathbf{f}_k|\mathbf{u}, \Theta) p(\mathbf{y}_k|\mathbf{f}_k, \Theta) d\mathbf{u} \end{aligned} \quad (6)$$

where the variational distribution $q(\mathbf{u})$ is part of the bound and explicitly parametrized as $q(\mathbf{u}) = \mathcal{N}(\mathbf{u}|\boldsymbol{\mu}, \boldsymbol{\Sigma})$. This uncollapsed bound satisfies $\mathcal{L}_{SVGP}(\boldsymbol{\mu}, \boldsymbol{\Sigma}, \Theta) \leq \mathcal{L}_{VFE}(\Theta)$ with equality when inserting the optimal mean and covariance of the variational distribution of VFE. The key property of this bound is that it can be written as a sum of K terms, which allows *Stochastic Variational Inference* (SVI, [14]). Unfortunately, collapsing the bound, i.e. inserting the optimal distribution, reintroduces dependencies between the observations, and eliminates the global parameter \mathbf{u} which is needed for SVI. Therefore, all variational parameters are numerically estimated by following the noisy gradients of a stochastic estimate of the lower bound \mathcal{L}_{SVGP} . By passing through the training data a sufficient number of times, the variational distribution converges to the batch solution of VFE method. However, the disadvantage of this approach is the large number of parameters, since in addition to the parameters Θ , all entries in the mean vector $\boldsymbol{\mu}$ and the covariance matrix $\boldsymbol{\Sigma}$ have to be estimated numerically, which is in order $\mathcal{O}(M^2)$.

3 Recursive Sparse GP Regression

In this section we establish the connection between Bayesian recursive estimation and sparse inducing point GP models. In a first step, we explicitly report for a large class of sparse inducing point GP models their *weight-space view* (see [27], Ch. 2.1) which can also

be seen as a particular kernelized version of a Bayesian linear regression model. In particular, we discuss the explicit choices of basis functions, the model specific observation noise, and the predictive transition distribution in a Bayesian kernelized linear regression model with additional input dependent observation noise for several sparse GP methods discussed by [27] for the batch case. Using these insights, we can exploit in a next step the recursive estimation algorithms known as the update equations of the *Kalman Filter* (KF) and *Information Filter* (IF) which allows to train many sparse methods analytically either in an online or distributed setting for given parameters. For the purpose of parameter estimation (which we will discuss in the next section), we discuss the recursive marginal log-likelihood with a model specific regularization term.

3.1 Weight-Space View of Generic Sparse GP

For any $\mathbf{X} \in \mathbb{R}^{B \times D}$, consider the generic sparse GP model

$$f(\mathbf{X}) = H(\mathbf{X})\mathbf{u} + \gamma(\mathbf{X}) \quad (7)$$

where the sparse GP value $f(\mathbf{X})$ is modeled by a linear combination of basis-functions $H(\mathbf{X}) \in \mathbb{R}^{B \times M}$, (stochastic) weights $\mathbf{u} \in \mathbb{R}^M$ with a prior $p(\mathbf{u}) = \mathcal{N}(\mathbf{0}, \boldsymbol{\Sigma}_0)$ and an input dependent error term $\gamma(\mathbf{X}) \sim \mathcal{N}(\mathbf{0}, V(\mathbf{X}))$ that takes into account the sparse approximation. For $k = 1, \dots, K$, the noisy observations \mathbf{y}_k are obtained by adding independent noise $\boldsymbol{\varepsilon}_k \sim \mathcal{N}(\mathbf{0}, \sigma_n^2 \mathbb{I})$ to $f(\mathbf{X}_k)$, yielding the model

$$\mathbf{y}_k = \mathbf{f}_k + \boldsymbol{\varepsilon}_k; \quad (8)$$

$$\mathbf{f}_k = \mathbf{H}_k \mathbf{u} + \gamma_k \quad \text{and} \quad \mathbf{f}_* = \mathbf{H}_* \mathbf{u} + \gamma_*, \quad (9)$$

where we explicitly distinguish the training $\mathbf{f}_k = f(\mathbf{X}_k)$ and test $\mathbf{f}_* = f(\mathbf{X}_*)$ cases depending on the input \mathbf{X}_k and \mathbf{X}_* . Assuming γ_k , γ_* and $\boldsymbol{\varepsilon}_k$ are independent, by linearity and Gaussianity we can compactly write

$$p(\mathbf{y}_k|\mathbf{f}_k) = \mathcal{N}(\mathbf{y}_k|\mathbf{f}_k, \sigma_n^2 \mathbb{I}); \quad (10)$$

$$p(\mathbf{u}) = \mathcal{N}(\mathbf{0}, \boldsymbol{\Sigma}_0); \quad (11)$$

$$p(\mathbf{f}_k|\mathbf{u}) = \mathcal{N}(\mathbf{f}_k|\mathbf{H}_k \mathbf{u}, \bar{\mathbf{V}}_k); \quad (12)$$

$$p(\mathbf{f}_*|\mathbf{u}) = \mathcal{N}(\mathbf{f}_*|\mathbf{H}_* \mathbf{u}, \mathbf{V}_*), \quad (13)$$

where $\bar{\mathbf{V}}_k$ and \mathbf{V}_* denote different covariances. Combining (10) and (12) by integrating out \mathbf{f}_k (40) gives rise

to the likelihood $p(\mathbf{y}_k|\mathbf{u}) = \mathcal{N}(\mathbf{y}_k|\mathbf{H}_k\mathbf{u}, \mathbf{V}_k)$ where $\mathbf{V}_k = \bar{\mathbf{V}}_k + \sigma_n^2\mathbb{I}$. Thus, the generic sparse GP model given by the prior together with this likelihood can be seen as a Bayesian non-linear regression model with additional input dependent observation noise with a particular choice of basis functions and covariance structure. For inducing inputs $\mathbf{R} \in \mathbb{R}^{M \times D}$, we explicit $\Sigma_0 = \mathbf{K}_{RR}$, $\mathbf{H}_k = \mathbf{K}_{X_k R} \mathbf{K}_{RR}^{-1}$ and $\mathbf{H}_* = \mathbf{K}_{*R} \mathbf{K}_{RR}^{-1}$. By different choices of the quantities $\bar{\mathbf{V}}_k$ and \mathbf{V}_* , a range of different sparse GP models are obtained. For fixed Θ , these models differ from each other only by the choice of the input dependent observation noise covariance $\bar{\mathbf{V}}_k$ and the prediction covariance \mathbf{V}_* . More concretely, for instance choosing $\bar{\mathbf{V}}_k^{\text{FITC}} = \text{Diag}[D_{X_k}]$, $\bar{\mathbf{V}}_k^{\text{VFE}} = \mathbf{0}$, $\bar{\mathbf{V}}_k^{\text{PEP}} = \alpha \text{Diag}[D_{X_k}]$ and $\mathbf{V}_* = D_*$, the sparse models FITC, VFE and PEP (see also Appendix B), respectively, are recovered. The details of different choices for more sparse models are summarized in the bottom table in Figure 2.

a) parameters			b) transformed parameters		
Σ_0	\mathbf{H}_k	\mathbf{H}_*	$\tilde{\Sigma}_0$	$\tilde{\mathbf{H}}_k$	$\tilde{\mathbf{H}}_*$
\mathbf{K}_{RR}	$\mathbf{K}_{X_k R} \mathbf{K}_{RR}^{-1}$	$\mathbf{K}_{*R} \mathbf{K}_{RR}^{-1}$	\mathbf{K}_{RR}^{-1}	$\mathbf{K}_{X_k R}$	\mathbf{K}_{*R}
	I) training	II) prediction	III) optimization		
	$\bar{\mathbf{V}}_k$	\mathbf{V}_*	a_k		
DIC	0	0	0		
DTC	0	D_*	0		
FITC	$\text{Diag}[D_{X_k}]$	D_*	0		
FIC	$\text{Diag}[D_{X_k}]$	$\text{Diag}[D_*]$	0		
PITC	D_{X_k}	D_*	0		
VFE	0	D_*	$\frac{1}{2\sigma_n^2} \text{Tr}[D_{X_k}]$		
PEP	$\alpha \text{Diag}[D_{X_k}]$	D_*	$\frac{1-\alpha}{2\alpha} \sum_i \log(1 + \frac{\alpha}{\sigma_n^2} D_{X_k}^{(i)})$		
PEP _B	αD_{X_k}	D_*	$\frac{1-\alpha_k}{2\alpha_k} \log I + \frac{\alpha}{\sigma_n^2} D_{X_k} $		

Figure 2: Summary of parameters for sparse GP models for recursive estimation. For all models, we have $\mu_0 = \mathbf{0}$, $\mathbf{V}_k = \bar{\mathbf{V}}_k + \sigma_n^2\mathbb{I}$ and Σ_0 , \mathbf{H}_k , \mathbf{H}_* from the table a) or a transformed version b). Using the model specific quantities for the observation noise $\bar{\mathbf{V}}_k$, the prediction covariance \mathbf{V}_* and the regularization term a_k from the bottom table allows the training with the recursive approaches. Consider the Section 3.1 for more details.

3.2 Training

After the prior $p(\mathbf{u})$ and the likelihood $p(\mathbf{y}_k|\mathbf{u})$ are specified in a Bayesian regression model, the posterior

over the weights \mathbf{u} conditioned on the data $\mathbf{y}_{1:k}$ can be computed either in a batch or in a recursive manner.

3.2.1 Batch Estimation

The batch likelihood is $p(\mathbf{y}|\mathbf{u}) = \prod_{k=1}^K p(\mathbf{y}_k|\mathbf{u}) = \mathcal{N}(\mathbf{y}|\mathbf{H}\mathbf{u}, \mathbf{V})$ with $\mathbf{H} = [\mathbf{H}_1^T, \dots, \mathbf{H}_K^T]^T \in \mathbb{R}^{N \times M}$ and \mathbf{V} a block-diagonal matrix with blocks \mathbf{V}_k . The posterior over \mathbf{u} given the data \mathbf{y} can be obtained by Bayes' rule, i.e.

$$p(\mathbf{u}|\mathbf{y}) \propto p(\mathbf{y}|\mathbf{u}) p(\mathbf{u}) \propto \mathcal{N}(\mathbf{u}|\boldsymbol{\mu}_K, \boldsymbol{\Sigma}_K), \quad (14)$$

with $\boldsymbol{\Sigma}_K = (\boldsymbol{\Sigma}_0^{-1} + \mathbf{H}^T \mathbf{V}^{-1} \mathbf{H})^{-1}$ and $\boldsymbol{\mu}_K = \boldsymbol{\Sigma}_K \mathbf{H}^T \mathbf{V}^{-1} \mathbf{y}$ where we used the standard linear Gaussian identity in (41).

3.2.2 Recursive Estimation

An equivalent solution can be obtained by propagating recursively $p(\mathbf{u}|\mathbf{y}_{1:k-1})$. By interpreting this previous posterior as the prior, the updated posterior can be recursively computed by

$$p(\mathbf{u}|\mathbf{y}_{1:k}) \propto p(\mathbf{y}_k|\mathbf{u}) p(\mathbf{u}|\mathbf{y}_{1:k-1}) \propto \mathcal{N}(\mathbf{u}|\boldsymbol{\mu}_k, \boldsymbol{\Sigma}_k), \quad (15)$$

where $\boldsymbol{\mu}_k = \boldsymbol{\Sigma}_k (\mathbf{H}_k^T \mathbf{V}_k^{-1} \mathbf{y}_k + \boldsymbol{\Sigma}_{k-1}^{-1} \boldsymbol{\mu}_{k-1})$ and $\boldsymbol{\Sigma}_k = (\boldsymbol{\Sigma}_{k-1}^{-1} + \mathbf{H}_k^T \mathbf{V}_k^{-1} \mathbf{H}_k)^{-1}$.

Kalman Filter like updating

The Kalman Filter [15] constitutes an efficient way to update the mean and covariance of $p(\mathbf{u}|\mathbf{y}_{1:k})$. Applying the matrix inversion lemma (38) to $\boldsymbol{\Sigma}_k$ in Eq. (15) and introducing temporary variables yields

$$\begin{aligned} \mathbf{r}_k &= \mathbf{y}_k - \mathbf{H}_k \boldsymbol{\mu}_{k-1}; \\ \mathbf{S}_k &= \mathbf{H}_k \boldsymbol{\Sigma}_{k-1} \mathbf{H}_k^T + \mathbf{V}_k; \\ \mathbf{G}_k &= \boldsymbol{\Sigma}_{k-1} \mathbf{H}_k^T \mathbf{S}_k^{-1}; \end{aligned} \quad \begin{aligned} \boldsymbol{\mu}_k &= \boldsymbol{\mu}_{k-1} + \mathbf{G}_k \mathbf{r}_k; \\ \boldsymbol{\Sigma}_k &= \boldsymbol{\Sigma}_{k-1} - \mathbf{G}_k \mathbf{S}_k \mathbf{G}_k^T. \end{aligned} \quad (16)$$

Starting the recursion with $\boldsymbol{\mu}_0 = \mathbf{0}$ and $\boldsymbol{\Sigma}_0$, the posterior distribution at step K is equivalent to (14) independent of the order of the data. We want to emphasize that the only difference in the estimation part between the sparse GP models is in the additional noise $\mathbf{V}_k = \bar{\mathbf{V}}_k + \sigma_n^2\mathbb{I}$.

Information Filter like updating

Using the natural parameter representation of a Gaussian $\mathcal{N}^{-1}(\mathbf{u}|\boldsymbol{\eta}_k, \boldsymbol{\Lambda}_k) = \mathcal{N}^{-1}(\mathbf{u}|\boldsymbol{\Sigma}_k^{-1}\boldsymbol{\mu}_k, \boldsymbol{\Sigma}_k^{-1})$, it directly follows from (15) that the posterior $p(\mathbf{u}|\mathbf{y}_{1:k})$ can be recursively computed

$$\begin{aligned}\boldsymbol{\eta}_k &= \boldsymbol{\eta}_{k-1} + \mathbf{H}_k^T \mathbf{V}_k^{-1} \mathbf{y}_k; \\ \boldsymbol{\Lambda}_k &= \boldsymbol{\Lambda}_{k-1} + \mathbf{H}_k^T \mathbf{V}_k^{-1} \mathbf{H}_k,\end{aligned}\quad (17)$$

with $\boldsymbol{\eta}_0 = \mathbf{0}$ and $\boldsymbol{\Lambda}_0 = \boldsymbol{\Sigma}_0^{-1}$. For any k , it holds $\boldsymbol{\mu}_k = \boldsymbol{\Lambda}_k^{-1} \boldsymbol{\eta}_k$ and $\boldsymbol{\Sigma}_k = \boldsymbol{\Lambda}_k^{-1}$. We can also write

$$\boldsymbol{\eta}_k = \sum_{k=1}^K \Delta \boldsymbol{\eta}_k \quad \text{and} \quad \boldsymbol{\Lambda}_k = \boldsymbol{\Lambda}_0 + \sum_{k=1}^K \Delta \boldsymbol{\Lambda}_k, \quad (18)$$

where $\Delta \boldsymbol{\eta}_k = \mathbf{H}_k^T \mathbf{V}_k^{-1} \mathbf{y}_k$ and $\Delta \boldsymbol{\Lambda}_k = \mathbf{H}_k^T \mathbf{V}_k^{-1} \mathbf{H}_k$. It is interesting to observe that $\Delta \boldsymbol{\eta}_k$ and $\Delta \boldsymbol{\Lambda}_k$ are independent of any other $\Delta \boldsymbol{\eta}_j$ or $\Delta \boldsymbol{\Lambda}_j$.

Whether using the KF or IF for the recursive computation of the sparse posterior depends on the the number of inducing points M and the size of the mini-batches B . If the number of inducing points is larger than the size of the mini-batches, i.e. $M > B$, the KF is cheaper, since only the matrix \mathbf{S}_k of size B has to be inverted, which is inexpensive regarding to the number of inducing points M . On the other hand, if $B > M$ (and assuming \mathbf{V} diagonal), the recursive IF approach is computationally cheaper since the inversion of the posterior precision is inexpensive regarding to the size of the mini-batch.

Transformation

Instead of running a KF with $\boldsymbol{\Sigma}_0 = \mathbf{K}_{RR}$, $\mathbf{H}_k = \mathbf{K}_{X_k R} \mathbf{K}_{RR}^{-1}$ and $\mathbf{H}_* = \mathbf{K}_{*R} \mathbf{K}_{RR}^{-1}$, an equivalent predictive distribution is also obtained when using $\tilde{\boldsymbol{\Sigma}}_0 = \mathbf{K}_{RR}^{-1}$ and $\tilde{\mathbf{H}}_k = \mathbf{K}_{X_k R}$ together with $\tilde{\mathbf{H}}_* = \mathbf{K}_{*R}$. For any k we then propagate a transformed posterior distribution $\tilde{\boldsymbol{\mu}}_k = \mathbf{K}_{RR}^{-1} \boldsymbol{\mu}_k$, $\tilde{\boldsymbol{\Sigma}}_k = \mathbf{K}_{RR}^{-1} \boldsymbol{\Sigma}_k \mathbf{K}_{RR}^{-1}$ and $\boldsymbol{\mu}_k = \mathbf{K}_{RR} \tilde{\boldsymbol{\mu}}_k$, $\boldsymbol{\Sigma}_k = \mathbf{K}_{RR} \tilde{\boldsymbol{\Sigma}}_k \mathbf{K}_{RR}$, respectively. For IF we apply an equivalent transformation, using $\tilde{\boldsymbol{\Lambda}}_0 = \mathbf{K}_{RR}$, $\tilde{\mathbf{H}}_k$ and $\tilde{\mathbf{H}}_*$ which results in propagating $\tilde{\boldsymbol{\eta}}_k = \mathbf{K}_{RR} \boldsymbol{\eta}_k$, $\tilde{\boldsymbol{\Lambda}}_k = \mathbf{K}_{RR} \boldsymbol{\Lambda}_k \mathbf{K}_{RR}$.

This parametrization constitutes a computational shortcut, since the basis functions are very easy to interpret and do not include any matrix multiplication. Note that also the log marginal likelihood discussed below is not affected by this transformation.

3.3 Prediction

Given a new $\mathbf{X}_* \in \mathbb{R}^{B \times D}$, the predictive distribution after seeing $\mathbf{y}_{1:k}$ of the sparse GP methods can be obtained

by

$$\begin{aligned}p(\mathbf{f}_*|\mathbf{y}_{1:k}) &= \int p(\mathbf{f}_*|\mathbf{u}) p(\mathbf{u}|\mathbf{y}_{1:k}) d\mathbf{u} \\ &= \mathcal{N}(\mathbf{f}_*|\mathbf{H}_* \boldsymbol{\mu}_k, \mathbf{H}_* \boldsymbol{\Sigma}_k \mathbf{H}_*^T + \mathbf{V}_*)\end{aligned}\quad (19)$$

using $p(\mathbf{f}_*|\mathbf{u}) = \mathcal{N}(\mathbf{f}_*|\mathbf{H}_* \mathbf{u}, \mathbf{V}_*)$ with $\mathbf{H}_* = \mathbf{K}_{*R} \mathbf{K}_{RR}^{-1}$ and \mathbf{V}_* the model specific prediction covariance. The predictions for \mathbf{y}^* are obtained by adding $\sigma_n^2 \mathbb{I}$ to the covariance of $\mathbf{f}_*|\mathbf{y}_{1:k}$. At step K , by applying (38) to the batch covariance $\boldsymbol{\Sigma}_K$ in (14), we get for the predictive distribution in (19)

$$\begin{aligned}\boldsymbol{\mu}_K^* &= \mathbf{H}_* \boldsymbol{\Sigma}_0 \mathbf{H}_*^T \boldsymbol{\Sigma} \mathbf{y}, \\ \boldsymbol{\Sigma}_K^* &= \mathbf{H}_* \boldsymbol{\Sigma}_0 \mathbf{H}_*^T - \mathbf{H}_* \boldsymbol{\Sigma}_0 \mathbf{H}_*^T \boldsymbol{\Sigma} \mathbf{H}_* \boldsymbol{\Sigma}_0 \mathbf{H}_*^T + \mathbf{V}_*,\end{aligned}\quad (20)$$

where $\boldsymbol{\Sigma} = (\mathbf{H} \boldsymbol{\Sigma}_0 \mathbf{H}^T + \mathbf{V})^{-1}$. Inserting the particular choices for $\boldsymbol{\Sigma}_0$, \mathbf{H} and \mathbf{H}_* yields the usual formulation for the sparse predictive distribution

$$\begin{aligned}\boldsymbol{\mu}_K^* &= \mathbf{Q}_{*X} (\mathbf{Q}_{XX} + \mathbf{V})^{-1} \mathbf{y}; \\ \boldsymbol{\Sigma}_K^* &= \mathbf{Q}_{**} - \mathbf{Q}_{*X} (\mathbf{Q}_{XX} + \mathbf{V})^{-1} \mathbf{Q}_{X*} + \mathbf{V}_*.\end{aligned}\quad (21)$$

Depending on the choice of the covariances $\bar{\mathbf{V}}$ and \mathbf{V}_* , we obtain for instance (3), (42) or (45) for PEP, VFE and FITC, respectively.

3.4 Marginal Likelihood

For model selection (or hyperparameters estimation) in the batch setting, the log marginal likelihood $\log p(\mathbf{y})$ of a Bayesian regression model can be computed by marginalizing out \mathbf{u} , that is

$$\begin{aligned}\log p(\mathbf{y}) &= \log \int p(\mathbf{y}|\mathbf{u}) p(\mathbf{u}) d\mathbf{u} \\ &= \log \mathcal{N}(\mathbf{y}|\mathbf{0}, \mathbf{H} \boldsymbol{\Sigma}_0 \mathbf{H}^T + \mathbf{V}).\end{aligned}\quad (22)$$

For the recursive setting, $p(\mathbf{y})$ can be factorized into $\prod_{k=1}^K p(\mathbf{y}_k|\mathbf{y}_{1:k-1})$, where the relative marginal likelihood is given by

$$\begin{aligned}p(\mathbf{y}_k|\mathbf{y}_{1:k-1}) &= \mathcal{N}(\mathbf{y}_k|\mathbf{H}_k \boldsymbol{\mu}_{k-1}, \mathbf{H}_k \boldsymbol{\Sigma}_{k-1} \mathbf{H}_k^T + \mathbf{V}_k) \\ &= \mathcal{N}(\mathbf{r}_k|\mathbf{0}, \mathbf{S}_k).\end{aligned}\quad (23)$$

The log of the joint marginal likelihood involving all terms of (23) can be explicitly written as

$$\begin{aligned}\log \prod_{k=1}^K p(\mathbf{y}_k|\mathbf{y}_{1:k-1}) &= \sum_{k=1}^K \log \mathcal{N}(\mathbf{r}_k|\mathbf{0}, \mathbf{S}_k) \\ &= -\frac{N}{2} \log 2\pi - \frac{1}{2} \sum_{k=1}^K \log |\mathbf{S}_k| + \mathbf{r}_k^T \mathbf{S}_k^{-1} \mathbf{r}_k.\end{aligned}\quad (24)$$

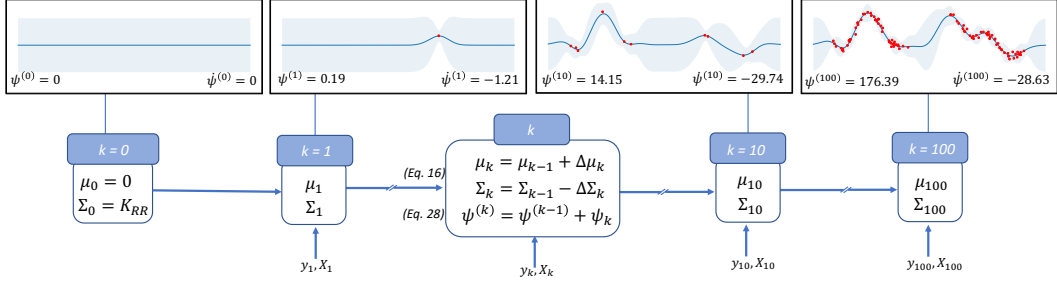


Figure 3: Online learning for the toy example in Section 3.5.1 for fixed Θ with batch size $B = 1$. In each step k , the sample $\mathbf{y}_k, \mathbf{X}_k$ is updated to the current posterior represented by $\boldsymbol{\mu}_k$ and $\boldsymbol{\Sigma}_k$ according to Eq. (16) together with the cumulative recursive bound $\Psi^{(k)}$ (Eq. (28)) and the numbers in the left corners of the plots). For recursive parameter estimation as discussed in Section 4.1, in addition to the posterior and the cumulative bound, the recursive derivatives of these quantities are propagated similarly for each k . The derivatives of this bound w.r.t. to the lengthscales are indicated in the right corners of the plots. Note, the cumulative bound and its derivative at step $k = 100$ are exactly the same as in the corresponding batch version in Figure 1.

By maximizing iteratively a lower bound of the recursive factorized marginal likelihood in (23) leads to the recursive KF updates in (16) for the posterior and the resulting lower bound

$$\psi(\Theta) = \sum_{k=1}^K \log \mathcal{N}(\mathbf{r}_k^\Theta | \mathbf{0}, \mathbf{S}_k^\Theta) - a_k(\Theta) \quad (25)$$

includes a model specific regularization term a_k (consider the corresponding column in Figure 2). We refer to this as the *recursive collapsed bound* and a detailed derivation for the VFE model is given in Appendix D. Using the model specific quantities $\bar{\mathbf{V}}_k$ and a_k , this recursive computation of the lower bound of the marginal likelihood are equivalent to the batch counterparts for all sparse models, for instance (5) and (4) for VFE and PEP, respectively.

Compared to the collapsed bound in (5), our recursive collapsed bound in (25) decomposes into a recursive sum over the mini-batches which allows to optimize the hyperparameters Θ sequentially. The advantage, compared to the uncollapsed bound in (6), is that the variational distribution is recursively and analytically eliminated, thus reducing the number of parameters to be numerically estimated drastically from $\mathcal{O}(MD + M^2)$ to $\mathcal{O}(MD)$.

3.5 Online and Distributed Learning

The connection between sparse GP models and recursive estimation established in the previous sections allows us to train the sparse GP models analytically either online for streaming data or in a distributed setting for fixed Θ . In the first case, we propagate either the mean $\boldsymbol{\mu}_k$ and covariance $\boldsymbol{\Sigma}_k$ (16) or the natural mean $\boldsymbol{\eta}_k$ and precision $\boldsymbol{\Lambda}_k$ (17) (depending on B and M) of the current posterior for each k recursively. In the second case we compute $\boldsymbol{\eta}_k$ and $\boldsymbol{\Lambda}_k$ (18) distributed among K computational nodes, and aggregate afterwards centralized the joint full posterior $\boldsymbol{\mu}_K, \boldsymbol{\Sigma}_K$. At step K , after seeing each sample once, we get exactly the same distribution for the inducing outputs and the same predictive distribution as the corresponding batch counterparts. In particular, exploiting the transformation from the Section 3.2.2 allows efficient online and distributed inference.

Suppose we have $N = 100$ data samples in $D = 1$ (only for illustration purposes, it works as well as for more dimensions) and we want to use the PEP model with $\alpha = 0.5$ with $M = 15$ inducing points. We show on a toy example the above proposed online and distributed learning procedures for sparse GPs when Θ is available in advance.

3.5.1 Online Setting

Assuming the data samples $\{\mathbf{x}_k, y_k\}$ arrive sequentially in a stream. Thus we have $B = 1$ and $K = 100$. Using the transformation, we have $\tilde{\mathbf{h}}_k = \mathbf{K}_{\mathbf{x}_k \mathbf{R}} \in \mathbb{R}^{1 \times 15}$

and $v_k = \alpha d_{x_k} + \sigma_n^2 \in \mathbb{R}$ and we set $\tilde{\Sigma}_0$ to \mathbf{K}_{RR}^{-1} . For each data sample k we compute the residual $r_k = y_k - \tilde{\mathbf{h}}_k \tilde{\boldsymbol{\mu}}_{k-1} \in \mathbb{R}$, the innovation variance $s_k = \tilde{\mathbf{h}}_k \tilde{\Sigma}_{k-1} \tilde{\mathbf{h}}_k^T + v_k \in \mathbb{R}$ and the Kalman gain $\tilde{\mathbf{g}}_k = \tilde{\Sigma}_{k-1} \tilde{\mathbf{h}}_k^T / s_k \in \mathbb{R}^{15}$. The (transformed) posterior distribution over the inducing points can then be updated by

$$\tilde{\boldsymbol{\mu}}_k = \tilde{\boldsymbol{\mu}}_{k-1} + \tilde{\mathbf{g}}_k r_k \quad \text{and} \quad \tilde{\Sigma}_k = \tilde{\Sigma}_{k-1} - s_k \tilde{\mathbf{g}}_k \tilde{\mathbf{g}}_k^T. \quad (26)$$

In order to make predictions for new data \mathbf{X}_* , we use $\tilde{\mathbf{H}}_* = \mathbf{K}_{*R}$ and $\mathbf{V}_* = \mathbf{K}_{*R} \mathbf{K}_{RR}^{-1} \mathbf{K}_{R*}$ and apply (19). Note that there is no need to transform back the posterior over the inducing points, since it is already taken into account in the prediction step. After processing all N samples, the predictive distribution and the cumulative bound of marginal log-likelihood correspond to the batch version, which is depicted in Figure 3.

3.5.2 Distributed Setting

Assuming the data is available in a batch, but we want to distribute the computation among $K = 4$ computational nodes, thus we have $B = 25$. Using the transformation, we have $\tilde{\mathbf{\Lambda}}_0 = \mathbf{K}_{RR}$, $\tilde{\mathbf{H}}_k = \mathbf{K}_{\mathbf{X}_k R} \in \mathbb{R}^{25 \times 15}$, $\mathbf{V}_k = \text{Diag}[\mathbf{v}_k] \in \mathbb{R}^{25 \times 25}$ where $\mathbf{v}_k = \alpha(\text{diag}[\mathbf{D}_{\mathbf{X}_k}] + \sigma_n^2)$. Each node now computes

$$\begin{aligned} \Delta \tilde{\boldsymbol{\eta}}_k &= \tilde{\mathbf{H}}_k^T \mathbf{V}_k^{-1} \mathbf{y}_k = \mathbf{K}_{R\mathbf{X}_k} \text{Diag}[\mathbf{v}_k^{-1}] \mathbf{y}_k, \\ \Delta \tilde{\mathbf{\Lambda}}_k &= \tilde{\mathbf{H}}_k^T \mathbf{V}_k^{-1} \tilde{\mathbf{H}}_k = \mathbf{K}_{R\mathbf{X}_k} \text{Diag}[\mathbf{v}_k^{-1}] \mathbf{K}_{\mathbf{X}_k R}. \end{aligned}$$

Afterwards, we sum up at a central node the (transformed) posterior distribution over the inducing points with $\tilde{\boldsymbol{\eta}}_K = \sum_{k=1}^4 \Delta \tilde{\boldsymbol{\eta}}_k$ and $\tilde{\mathbf{\Lambda}}_K = \tilde{\mathbf{\Lambda}}_0 + \sum_{k=1}^4 \Delta \tilde{\mathbf{\Lambda}}_k$, followed by $\tilde{\Sigma}_K = \tilde{\mathbf{\Lambda}}_K^{-1}$ and $\tilde{\boldsymbol{\mu}}_K = \tilde{\Sigma}_K \tilde{\boldsymbol{\eta}}_K$. Prediction can be done with $\tilde{\mathbf{H}}_*$ and \mathbf{V}_* as explained in the online setting. This procedure is illustrated in Figure 4. Note that the samples are only sorted for illustration purposes.

4 Hyperparameters Estimation

In the previous section we discussed online and distributed procedures for analytical computation of sparse GP models for fixed Θ where we recovered the batch solution after seeing each sample once. In this section we show how to exploit the connection to recursive estimation when optimizing Θ in a sequential or distributed way. Note that we only estimate these parameters and not all entries in the posterior mean vector and covariance matrix compared to SVGP where no analytic updates of these quantities are available.

In particular, we explain how to use the *recursive collapsed bound* in (28) by using recursive gradient propagation which enables the application of stochastic optimization. Moreover, we present an idea based on distributed gradient cumulation of the natural mean and precision with respect to the parameters Θ which allows to alternatively distribute the computations. Both these techniques can be applied to all sparse GP models discussed in Section 2.1.

Finding a maximizer for $\theta \in \Theta$ of an objective function $\varphi(\Theta) = \sum_{k=1}^K \varphi_k(\Theta)$ can be achieved by applying *Stochastic Gradient Descent* (SGD), where the update can be written as

$$\theta^{(t)} = \theta^{(t-1)} + \gamma^{(t-1)} \frac{\partial \varphi_k(\Theta)}{\partial \theta} \Big|_{\theta=\theta^{(t-1)}}, \quad (27)$$

where $\gamma^{(t-1)}$ might be a sophisticated function of $\theta^{(0)}, \dots, \theta^{(t-1)}$ (for instance using ADAM [16], where also a bias correction term is included). We call one pass over the K mini-batches an epoch. We denote $\theta^{(e,k)} \in \Theta^{(e,k)}$ the estimate of θ in epoch $e \in E$ for mini-batch k .

4.1 Recursive Gradient Propagation (RGP)

We recall the *recursive collapsed bound* in (25)

$$\psi^{(K)}(\Theta) = \sum_{k=1}^K d_k(\Theta) - a_k(\Theta) = \sum_{k=1}^K \psi_k(\Theta) \quad (28)$$

where $d_k(\Theta) = \log \mathcal{N}(\mathbf{r}_k^\Theta | \mathbf{0}, \mathbf{S}_k^\Theta)$ and $a_k(\Theta)$ the model specific regularization term. Since $\psi^{(K)}(\Theta)$ decomposes into a (recursive) sum over the mini-batches, we directly compute the derivative of $\psi_k(\Theta)$ w.r.t. $\theta \in \Theta$. The derivative of a_k is straightforward, for the former we can write

$$\frac{\partial d_k(\Theta)}{\partial \theta} = -\frac{1}{2} \frac{\partial \log |\mathbf{S}_k^\Theta|}{\partial \theta} - \frac{1}{2} \frac{\partial (\mathbf{r}_k^\Theta)^T (\mathbf{S}_k^\Theta)^{-1} \mathbf{r}_k^\Theta}{\partial \theta} \quad (29)$$

with $\mathbf{r}_k^\Theta = \mathbf{y}_k - \mathbf{H}_k^\Theta \boldsymbol{\Lambda}_{k-1}^{\Theta-1} \boldsymbol{\eta}_{k-1}^\Theta$ and $\mathbf{S}_k^\Theta = \mathbf{H}_k^\Theta \boldsymbol{\Lambda}_{k-1}^{\Theta-1} (\mathbf{H}_k^\Theta)^T + \mathbf{V}_k^\Theta$. It is important to note that ignoring naively the dependency of Θ through $\boldsymbol{\eta}_{k-1}^\Theta$ and $\boldsymbol{\Lambda}_{k-1}^{\Theta-1}$ completely forgets the past and thus results in overfitting the current mini-batch. In order to compute the derivatives of $\boldsymbol{\eta}_k^\Theta$ and $\boldsymbol{\Lambda}_k^\Theta$, we exploit

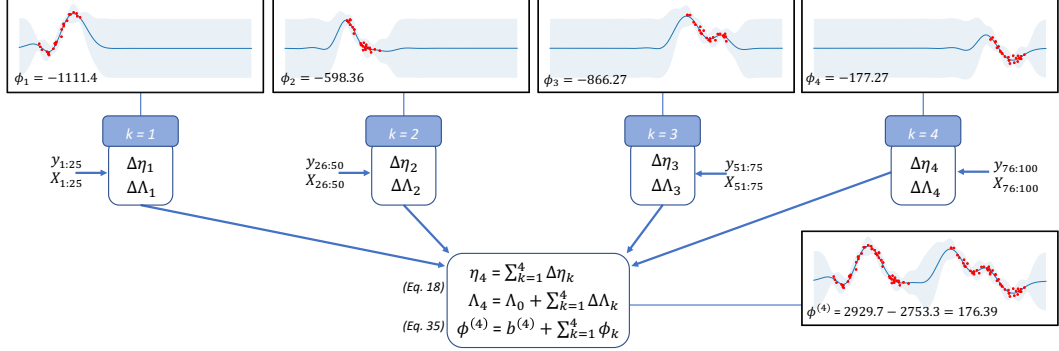


Figure 4: Distributed learning among $K = 4$ computational nodes for the toy example 3.5.2 for fixed Θ with mini-batch size $B = 25$. Each node k receives a mini-batch of data and computes the update for the posterior in the natural parameter space $\Delta\eta_k$ and $\Delta\Lambda_k$ defined below Eq. (18). In addition, the individual contribution $\Phi^{(k)}$ of the bound to the marginal likelihood is computed (indicated in left corners in the boxes). At a central node, the natural means, precision covariances and $\Phi^{(k)}$ are added together via (18) and (35). The resulting posterior and bound to the marginal likelihood are the same as in Figures 1 and 3.

the chain rule for derivatives and recursively propagate the gradients of the natural mean and the precision over time, that is

$$\frac{\partial \eta_k^\Theta}{\partial \theta} = \frac{\partial \eta_{k-1}^\Theta}{\partial \theta} + \frac{\partial \Delta\eta_k^\Theta}{\partial \theta} \quad \text{and} \quad \frac{\partial \Lambda_k^\Theta}{\partial \theta} = \frac{\partial \Lambda_{k-1}^\Theta}{\partial \theta} + \frac{\partial \Delta\Lambda_k^\Theta}{\partial \theta} \quad (30)$$

For simplicity, we show here the gradient propagation of the IF, depending on the B, M and D , it might be cheaper to use the KF to propagate recursively the gradients of the computations of μ_k and Σ_k in (16), that is

$$\begin{aligned} \frac{\partial \mathbf{u}_k}{\partial \theta} &= \frac{\partial \mathbf{u}_{k-1}}{\partial \theta} + \frac{\partial \mathbf{G}_k}{\partial \theta} \mathbf{r}_k + \mathbf{G}_k \frac{\partial \mathbf{r}_k}{\partial \theta} \\ \frac{\partial \Sigma_k}{\partial \theta} &= \frac{\partial \Sigma_{k-1}}{\partial \theta} - \frac{\partial \mathbf{G}_k}{\partial \theta} \mathbf{S}_k \mathbf{G}_k^T - \mathbf{G}_k \frac{\partial \mathbf{S}_k}{\partial \theta} \mathbf{G}_k - \mathbf{G}_k \mathbf{S}_k \frac{\partial \mathbf{G}_k^T}{\partial \theta}, \end{aligned} \quad (31)$$

where $\frac{\partial \mathbf{G}_k}{\partial \theta}$, $\frac{\partial \mathbf{r}_k}{\partial \theta}$ and $\frac{\partial \mathbf{S}_k}{\partial \theta}$ are computed recursively according to (16). Computing the derivatives of d_k as explained in (29) and (30)/(31), the stochastic gradient

$$\frac{\partial \psi_k(\Theta)}{\partial \theta} = \frac{\partial d_k(\Theta)}{\partial \theta} - \frac{\partial a_k(\Theta)}{\partial \theta} \quad (32)$$

can be computed for each mini-batch k . Suppose keeping Θ constant, the cumulative derivative at step K for the recursive collapsed bound is equal to the corresponding derivatives of the batch sparse bound, which can be verified for the toy example in Figure 3.

The numbers in the bottom left and right corners show the cumulative recursive collapsed bound $\psi^{(k)}$ and its cumulative derivative $\frac{\partial \psi^{(k)}}{\partial \mathbf{1}}$ (abbreviated as $\dot{\psi}^{(k)}$) with respect to the lengthscale, respectively. We get for the lower bound of the marginal likelihood as well as its derivatives exactly the same value as the corresponding batch counterpart in Figure 1.

For *Stochastic Recursive Gradient Propagation* (SRGP), in each epoch e and mini-batch k , we interleave the update step of the inducing points in Equation (15) with the SGD update (27) of the parameters $\Theta^{(e,k)}$, i.e.

$$\begin{aligned} p(\mathbf{u} | \mathbf{y}_{1:k}, \Theta^{(e,k)}) &\approx p(\mathbf{y}_k | \mathbf{u}, \Theta^{(e,k)}) \\ &\times p(\mathbf{u} | \mathbf{y}_{1:k-1}, \Theta^{(e,k-1)}). \end{aligned} \quad (33)$$

More concretely, we update after each mini-batch k the parameters $\Theta^{(e,k)}$ with (32),(27) and propagate recursively the posterior with (18) and its derivative (30). In order to compute all the derivatives with respect to $\theta \in \Theta$, we can exploit several matrix derivative rules which simplifies the computation significantly. A detailed algorithm is provided in the Appendix C.

In the following, we assume that the batch size B is larger than the number of inducing points M . For one mini-batch, the time complexity to update the posterior is dominated by matrix multiplications of size B and

M , thus $\mathcal{O}(B^2M)$. In order to propagate the gradients of the posterior and to compute the derivative of the bound needs $\mathcal{O}(BM^2)$ for a mini-batch and a parameter $\theta \in \Theta$. Thus, updating a mini-batch including all $\mathcal{O}(MD)$ parameters costs $\mathcal{O}(BM^3D + B^2M)$ for the SRGP method. Since SRGP stores the gradients of the posterior, it requires $\mathcal{O}(M^3D + BM)$ storage.

On the other hand, SVGP needs $\mathcal{O}(M^2 + BM)$ storage and $\mathcal{O}(BM^3 + B^2M)$ time per mini-batch, where the latter can be broken down into once $\mathcal{O}(B^2M)$ and $\mathcal{O}(BM)$ for each of the $\mathcal{O}(M^2)$ parameters. This means, for moderate dimensions, our algorithm has the same time complexity as state of the art method SVGP. However, due to the analytic updates of the posterior we achieve an higher accuracy and less epochs are needed which can be confirmed in Figure 5 and in Section 5 empirically.

Figure 5 shows the convergence of SRGP on a 1-D toy example with $N = 1000$ data samples and $M = 15$ inducing points. The parameters are sequentially optimized with our recursive approach (blue) and as comparison with SVGP (green) with a mini-batch size of $B = 100$ over several epochs. The root-mean-squared-error (RMSE) computed on test points, the bound of the log-marginal likelihood (LML) as well as the hyperparameters converge in a few iterations to the corresponding batch values of VFE (red). Due to the analytic updates of the posterior, the accuracy is higher and SRGP needs much less epochs until convergence.

4.2 Distributed Gradient Cumulation

Instead of recursively propagating the derivatives (30), we outline an approach to distribute the computations. By applying (38) and (39) to $\mathbf{H}\Sigma_0\mathbf{H}^T + \mathbf{V}$ in (22), the batch marginal log likelihood can also be written in terms of the posterior mean and covariance, that is

$$\begin{aligned} \log p(\mathbf{y}) = & -\frac{1}{2} \log |\Sigma_0| + \frac{1}{2} \log |\Sigma_K| + \frac{1}{2} \boldsymbol{\mu}_K^T \Sigma_K^{-1} \boldsymbol{\mu}_K \\ & + \sum_{k=1}^K \log \mathcal{N}(\mathbf{y}_k | \mathbf{0}, \mathbf{V}_k), \end{aligned} \quad (34)$$

where we can observe that it decomposes into a local term for each mini-batch and a global term involving the prior and posterior. In order to match the sparse GP bounds, similarly as in (28), a model specific regular-

ization term a_k has to be subtracted, leading to

$$\begin{aligned} \phi^{(K)}(\Theta) &= \frac{1}{2} b^{(K)}(\Theta) + \sum_{k=1}^K c_k(\Theta) - a_k(\Theta) \\ &= \frac{1}{2} b^{(K)}(\Theta) + \sum_{k=1}^K \phi_k(\Theta) \end{aligned} \quad (35)$$

where we define $c_k(\Theta) = \log \mathcal{N}(\mathbf{y}_k | \mathbf{0}, \mathbf{V}_k^\Theta)$, $\phi_k = c_k - a_k$ and $b^{(K)}(\Theta) = -\log |\Sigma_0^\Theta| + \log |\Sigma_K^\Theta| + (\boldsymbol{\mu}_K^\Theta)^T (\Sigma_K^\Theta)^{-1} \boldsymbol{\mu}_K^\Theta$. The derivatives of ϕ_k can be computed straightforwardly in a distributed regime. Taking derivative of $b^{(K)}$ w.r.t. $\theta \in \Theta$ yields

$$\begin{aligned} \frac{\partial b^{(K)}(\Theta)}{\partial \theta} = & -\text{Tr} \left[\Lambda_0^\Theta \frac{\partial \Sigma_0^\Theta}{\partial \theta} \right] - \text{Tr} \left[\Sigma_K^\Theta \frac{\partial \Lambda_K^\Theta}{\partial \theta} \right] \\ & - (\boldsymbol{\mu}_K^\Theta)^T \frac{\partial \Lambda_K^\Theta}{\partial \theta} \boldsymbol{\mu}_K^\Theta + 2(\boldsymbol{\mu}_K^\Theta)^T \frac{\partial \boldsymbol{\eta}_K^\Theta}{\partial \theta}. \end{aligned} \quad (36)$$

In order to compute the the derivative of $b^{(K)}$, we can use the decomposition in (18), which leads to

$$\frac{\partial \boldsymbol{\eta}_K^\Theta}{\partial \theta} = \sum_{k=1}^K \frac{\partial \Delta \boldsymbol{\eta}_k^\Theta}{\partial \theta} \quad \text{and} \quad \frac{\partial \Lambda_K^\Theta}{\partial \theta} = \frac{\partial \Lambda_0^\Theta}{\partial \theta} + \sum_{k=1}^K \frac{\partial \Delta \Lambda_k^\Theta}{\partial \theta},$$

which can be distributed. Thus, we can compute $\Delta \boldsymbol{\eta}_k$, $\Delta \Lambda_k$, a_k and c_k together with the derivatives $\frac{\partial \Delta \boldsymbol{\eta}_k}{\partial \theta}$, $\frac{\partial \Delta \Lambda_k}{\partial \theta}$, $\frac{\partial a_k}{\partial \theta}$ and $\frac{\partial c_k}{\partial \theta}$ distributed among K computational nodes. The most straight-forward approach is to cumulate these quantities at a central node which enables to compute the derivatives in (36) centralized. For this approach, when updating the parameters Θ after each distributed round, there is no approximation involved compared to the batch case. More sophisticated distributed schemes with less communication costs and tree structure are possible, however, since our focus in this work lies on stochastic sequential parameter estimation, we defer the investigation of distributed parameter optimization to future work.

5 Experiments

For the empirical evaluations and comparisons, we focus on the sequential parameter estimation procedure SRGP introduced in Section 4.1. In order to demonstrate the scalability and the accurate performance of our recursive learning algorithm for stochastic parameter learning in sparse GPs, we first provide experiments

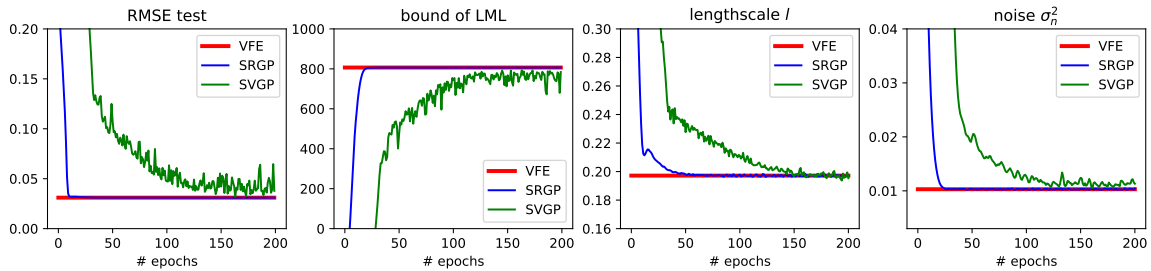


Figure 5: Convergence of SRGP (blue) on a 1-D toy to batch version VFE (red). Compared to SVGP (green), the convergence of the root-mean-squared-error (RMSE) of test points, the bound of the log-marginal likelihood (LML) as well as the hyperparameters is faster and more accurate.

based on $N = 100'000$ synthetic data samples generated by a GP in several dimensions. Next, we apply our approach to the Airline data used in [12] with a million of data samples. For a realistic scenario, we demonstrate how to use up to a million of data samples to train a nonlinear plant. We compare our SRGP method to full GP and sparse batch method VFE for a subset of data (using the implementation in GPy [10]) and to the state of the art stochastic parameter estimation method SVGP implemented in GPflow [20]. Note that our algorithm works also for many other sparse models, however, only large-scale implementations of standard SVGP are available (corresponding to the VFE model), thus we restrict the investigation to this model.

5.1 GP Simulation

In this section we test our proposed learning procedure on simulated GP data. We generate $N = 100'000$ data samples from a zero-mean (sparse) GP with SE covariance kernel with hyperparameters $\sigma_0 = 1, \sigma_n = 0.1$ and $l = \{0.1, 0.2, 0.5\}$ in $D = \{1, 2, 5\}$ dimensions. The initial $M = \{20, 50, 100\}$ inducing points are randomly selected from the data and the hyperparameters of a SE kernel with individual lengthscales for each dimension are initialized to the same values for both algorithms ($\sigma_0 = 1, \sigma_n = 1, l_1, \dots, l_D = 1$). All parameters are sequentially optimized with our recursive approach and as comparison with SVGP with a mini-batch size of $B = 5000$. The stochastic gradient descent method ADAM [16] is employed for both methods with learning rates $\{0.001, 0.005, 0.005\}$ for SVGP and $\{0.0001, 0.001, 0.005\}$ for SRGP (based on some preliminary experiments). Each experiment is replicated 10 times.

Figure 6 shows the bound to the log-marginal likeli-

hood, the RMSE and the coverage of $10'000$ test points for the data dimensions $D = \{1, 2, 5\}$ of both methods over 50 epochs. The shaded lines indicates the 10 repetitions and the thick line correspond to the mean. In all scenarios the recursive propagation of the gradients achieves faster convergence and more accurate performance regarding mean RMSE and smaller values for the log-marginal likelihood. We tried to set the learning rates as fair as possible, the accuracy and faster convergence can be explained by the analytic updates of the posterior mean and covariance which leads to less parameters to be optimized numerically.

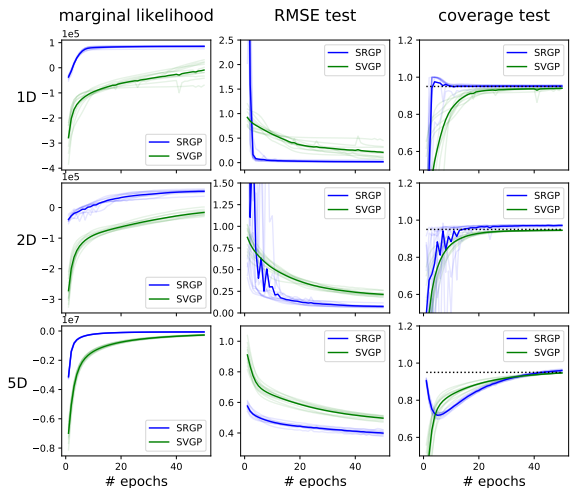


Figure 6: Convergence over 50 epochs for $N = 100'000$ synthetic GP data samples in several dimensions obtained by SVGP and our proposed method SRGP.

5.2 Airline Data

For the second example we apply our recursive method to the Airline Data used in [12]. It consists of flight arrival and departure times for more than 2 millions flights in the USA from January 2008 and April 2008. We preprocessed the data as similar as possible as described in [12] resulting in 8 variables: age of the aircraft, distance that needs to be covered, airtime, departure time, arrival time, day of the week, day of the month and month. We trained our recursive method as well as SVGP with an SE kernel on $N = 1'000'000$ data samples with $M = 500$ inducing points randomly selected from the data and a mini-batch size of $B = 10'000$. The ADAM learning rates are set to 0.005 for both methods and the size of the test set is $50'000$. For 5 different repetitions, the RMSE as a function of epochs is depicted in Figure 7. The performance of the recursive approach is superior than SVGP which demonstrates the accurate scalability of our approach for big-data.

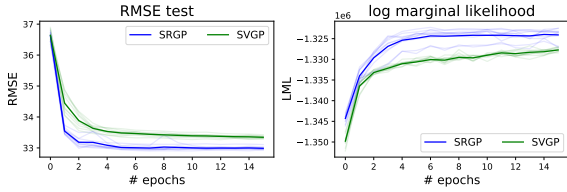


Figure 7: Convergence over several epochs of RMSE and bound to log marginal likelihood for $N = 1'000'000$ samples from the Airline data for SRGP and SVGP.

5.3 Non-Linear Plant

GPs are a powerful way to model complex functions in a non-parametric way, thus they are suitable to learn the complex input output behavior of a non-linear plant. However, with full or even sparse batch GP methods the use is restricted to a few thousands of samples. With our sequential learning method, we demonstrate how to exploit the huge amount of available data by training with up to a million of samples.

We consider a Continuous Stirred Tank Reactor

(CSTR). The dynamic model of the plant is

$$\begin{aligned} \frac{d}{dt}h(t) &= w_1(t) + w_2(t) - 0.2\sqrt{h(t)} \\ \frac{d}{dt}C_b(t) &= (C_{b1} - C_b(t))\frac{w_1(t)}{h(t)} + (C_{b2} - C_b(t))\frac{w_2(t)}{h(t)} \\ &\quad - \frac{k_1 C_b(t)}{(1 + k_2 C_b(t))^2} \end{aligned} \quad (37)$$

where $C_b(t)$ is the product concentration at the output of the process, $h(t)$ is the liquid level, $w_1(t)$ is the flow rate of concentrated feed C_{b1} , and $w_2(t)$ is the flow rate of the diluted feed C_{b2} . The input concentrations are $C_{b1} = 24.9$ and $C_{b2} = 0.1$. The constants associated with the rate of consumption are $k_1 = k_2 = 1$. The objective of the controller is to maintain the product concentration by changing the flow $w_1(t)$. To simplify the example, we assume that $w_2(t) = 0.1$ and that the level of the tank $h(t)$ is not controlled. We denote the controlled outputs $C_b(t), C_b(t-1), \dots, C_b(t-p)$ as $f_t, f_{t-1}, \dots, f_{t-p}$ and the control variables as $w_t, w_{t-1}, \dots, w_{t-p}$. Therefore, the plant identification problem can be shaped into the problem of estimating the non-linear function $f_t = g(f_{t-1}, \dots, f_{t-p}, w_t, w_{t-1}, \dots, w_{t-p})$ which depends on the p previous values as well as on the current and the p past control values w . However, we

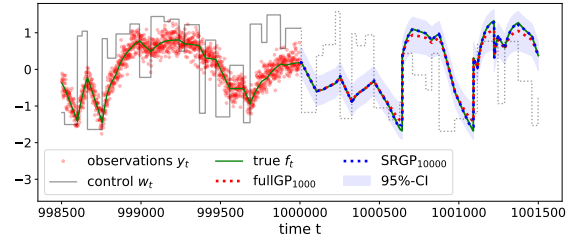


Figure 8: Training and prediction phases for non-linear plant.

can only observe a noisy version of the controlled response, that is $y_t = f_t + \varepsilon_t$ with $\varepsilon \sim \mathcal{N}(0, \sigma_n^2)$. Using a sampling rate of $0.2s$, we have generated $1'200'000$ observations (about 3 days of observations). The plant input is a series of steps, with random height (in the interval $[0, 4]$), occurring at random intervals (in the interval $[5, 20]s$). For different numbers N_{train} , we use the samples $y_{10^6 - N_{train}}, \dots, y_{10^6}$ for training and the last $200'000$ are used as a test set. The goal is to learn a model for the controlled response y_t given $\mathbf{x}_t = [y_{t-1}, y_{t-2}, w_t, w_{t-1}, w_{t-2}]^T \in \mathbb{R}^5$ for the particular choice of $p = 2$. We model the non-linear function g

with a GP with a SE kernel. For comparison, we train full GP and sparse batch GP (with 100 inducing points) on a time horizon N_{train} of up to 10'000 and 50'000 past values, respectively. With the sequential version SVGP and our recursive gradient propagation method SRGP (both with 100 inducing points and mini-batch size of 1'000), we use a time horizon of up to a million. This situation is depicted in Figure 8, where for 1500 training samples y_t (red dots), the true (unknown) function f_t (green) and the control input w_t (grey) is shown together with the predicted values with full GP (red dotted) and recursive GP (blue dotted) trained on a time horizon of 1'000 and 10'000, respectively. In Figure 9, the RMSE and the median computed on the test set (with 10 repetitions) is depicted for full GP, sparse GP (VFE), SVGP and SRGP trained with varying time horizons. For small and medium training sizes, when the batch methods are applicable, our recursive method achieves the same performance as the batch counterpart (VFE) and is comparable to full GP. Due to the analytic updates of the posterior, Rec outperforms SVGP regarding both RMSE and median for all training sizes. By exploiting more than several thousand past values, a significant increase in performance of SRGP can be still observed, thus it constitutes an approach to accurately scale GPs up to a million of past values.

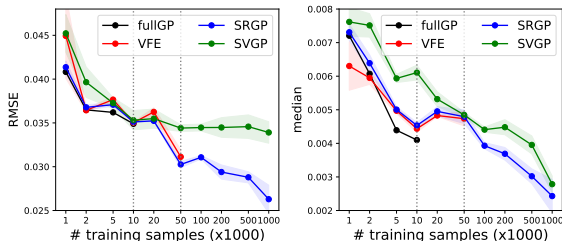


Figure 9: Performance (RMSE and median) for full GP, batch sparse GP (VFE), sequential SVGP, and our recursive method (SRGP) trained on varying time horizons (logarithmic scale). The grey dotted vertical lines at 10'000 and 50'000 indicate the maximal number of samples used for training with full GP and sparse batch GP (VFE), respectively.

6 Conclusion

In this paper we introduced a recursive inference and parameter estimation method SRGP for a general class

of sparse GP approximations. Since the posterior updates are given analytically, one pass through the data is sufficient to compute the posterior for given parameters. For parameter estimation, we proposed a recursive collapsed bound to the marginal likelihood that matches exactly the batch version but can be used for stochastic estimation. Due to the analytic updates of the posterior our method has much less parameters to be estimated numerically. As a consequence, the experimental section showed that our recursive method needs less epochs and has superior accuracy compared to state of the art, thus constitutes an efficient methodology for scaling GPs to big data problems.

Our approach could be enhanced in several directions. While the proposed method only exploits the update equations of the KF and IF, respectively, an interesting direction would be to include a dynamic in a state space model that takes into account the varying hyperparameters which makes it also applicable for the streaming setting as [4]. Moreover, we further plan to investigate distributed parameter estimation as outlined in Section 4.2.

Acknowledgments This work is supported by the Swiss National Research Programme 75 "Big Data" (NRP 75) with grant number 167199.

References

- [1] David Barber and Yali Wang. Gaussian processes for bayesian estimation in ordinary differential equations. In *ICML*, 2014.
- [2] Alessio Benavoli and Marco Zaffalon. State space representation of non-stationary gaussian processes. 2016.
- [3] Hildo Bijl, Thomas B. Schön, Jan-Willem van Wingerden, and Michel Verhaegen. Online sparse gaussian process training with input noise. *CoRR*, abs/1601.08068, 2016.
- [4] Thang D Bui, Cuong Nguyen, and Richard E Turner. Streaming sparse gaussian process approximations. In *Advances in Neural Information Processing Systems*, pages 3301–3309, 2017.
- [5] Thang D Bui, Josiah Yan, and Richard E Turner. A unifying framework for sparse gaussian process approximation using power expectation prop-

- agation. *Journal of Machine Learning Research*, 18:1–72, 2017.
- [6] Andrea Carron, Marco Todescato, Ruggero Carli, Luca Schenato, and Gianluigi Pillonetto. Machine learning meets kalman filtering. In *2016 IEEE 55th Conference on Decision and Control (CDC)*, pages 4594–4599. IEEE, 2016.
- [7] Tianshi Chen, Henrik Ohlsson, and Lennart Ljung. On the estimation of transfer functions, regularizations and gaussian processes—revisited. *Automatica*, 48(8):1525–1535, 2012.
- [8] Lehel Csató and Manfred Opper. Sparse online gaussian processes. *Neural computation*, 14(3):641–668, 2002.
- [9] Roger Frigola, Fredrik Lindsten, Thomas B Schön, and Carl Edward Rasmussen. Bayesian inference and learning in gaussian process state-space models with particle mcmc. In *Advances in Neural Information Processing Systems*, pages 3156–3164, 2013.
- [10] GPY. GPY: A gaussian process framework in python. <http://github.com/SheffieldML/GPY>, since 2012.
- [11] Jouni Hartikainen and Simo Särkkä. Kalman filtering and smoothing solutions to temporal gaussian process regression models. In *2010 IEEE International Workshop on Machine Learning for Signal Processing*, pages 379–384. IEEE, 2010.
- [12] James Hensman, Nicolo Fusi, and Neil D Lawrence. Gaussian processes for big data. In *Conference for Uncertainty in Artificial Intelligence*, 2013.
- [13] Trong Nghia Hoang, Quang Minh Hoang, and Bryan Kian Hsiang Low. A unifying framework of anytime sparse gaussian process regression models with stochastic variational inference for big data. In *ICML*, pages 569–578, 2015.
- [14] Matthew D Hoffman, David M Blei, Chong Wang, and John Paisley. Stochastic variational inference. *The Journal of Machine Learning Research*, 14(1):1303–1347, 2013.
- [15] Rudolph Emil Kalman et al. A new approach to linear filtering and prediction problems. *Journal of basic Engineering*, 82(1):35–45, 1960.
- [16] Diederik P Kingma and Jimmy Ba. Adam: A method for stochastic optimization. *arXiv preprint arXiv:1412.6980*, 2014.
- [17] Juš Kocijan, Agathe Girard, Blaž Banko, and Roderick Murray-Smith. Dynamic systems identification with gaussian processes. *Mathematical and Computer Modelling of Dynamical Systems*, 11(4):411–424, 2005.
- [18] Haitao Liu, Yew-Soon Ong, Xiaobo Shen, and Jianfei Cai. When gaussian process meets big data: A review of scalable gps. *arXiv preprint arXiv:1807.01065*, 2018.
- [19] Benn Macdonald, Catherine Higham, and Dirk Husmeier. Controversy in mechanistic modelling with gaussian processes. In *Proceedings of the 32Nd International Conference on International Conference on Machine Learning - Volume 37, ICML’15*, pages 1539–1547. JMLR.org, 2015.
- [20] Alexander G. de G. Matthews, Mark van der Wilk, Tom Nickson, Keisuke Fujii, Alexis Boukouvalas, Pablo León-Villagrà, Zoubin Ghahramani, and James Hensman. GPflow: A Gaussian process library using TensorFlow. *Journal of Machine Learning Research*, 18(40):1–6, apr 2017.
- [21] Csar Lincoln C. Mattos, Zhenwen Dai, Andreas Damianou, Jeremy Forth, Guilherme A. Barreto, and Neil D. Lawrence. Recurrent Gaussian processes. In Hugo Larochelle, Brian Kingsbury, and Samy Bengio, editors, *Proceedings of the International Conference on Learning Representations*, volume 3, Caribe Hotel, San Juan, PR, 00 2016.
- [22] Hao Peng, Shandian Zhe, Xiao Zhang, and Yuan Qi. Asynchronous distributed variational gaussian process for regression. In *Proceedings of the 34th International Conference on Machine Learning - Volume 70*, pages 2788–2797. JMLR. org, 2017.
- [23] Gianluigi Pillonetto. A new kernel-based approach to hybrid system identification. *Automatica*, 70:21–31, 2016.
- [24] Gianluigi Pillonetto and Giuseppe De Nicolao. A new kernel-based approach for linear system identification. *Automatica*, 46(1):81–93, 2010.

- [25] Gianluigi Pillonetto, Francesco Dinuzzo, Tianshi Chen, Giuseppe De Nicolao, and Lennart Ljung. Kernel methods in system identification, machine learning and function estimation: A survey. *Automatica*, 50(3):657–682, 2014.
- [26] Joaquin Quiñonero-Candela and Carl Edward Rasmussen. A unifying view of sparse approximate gaussian process regression. *Journal of Machine Learning Research*, 6(Dec):1939–1959, 2005.
- [27] Carl Edward Rasmussen and Christopher KI Williams. *Gaussian processes for machine learning*, volume 1. MIT press Cambridge, 2006.
- [28] Simo Sarkka, Arno Solin, and Jouni Hartikainen. Spatiotemporal learning via infinite-dimensional bayesian filtering and smoothing: A look at gaussian process regression through kalman filtering. *IEEE Signal Processing Magazine*, 30(4):51–61, 2013.
- [29] Matthias Seeger, Christopher Williams, and Neil Lawrence. Fast forward selection to speed up sparse gaussian process regression. In *Artificial Intelligence and Statistics 9*, number EPFL-CONF-161318, 2003.
- [30] Bernhard W Silverman. Some aspects of the spline smoothing approach to non-parametric regression curve fitting. *Journal of the Royal Statistical Society. Series B (Methodological)*, pages 1–52, 1985.
- [31] Alex J Smola and Peter L Bartlett. Sparse greedy gaussian process regression. In *Advances in neural information processing systems*, pages 619–625, 2001.
- [32] Edward Snelson and Zoubin Ghahramani. Sparse gaussian processes using pseudo-inputs. In *Advances in Neural Information Processing Systems*, pages 1257–1264, 2006.
- [33] Andreas Svensson and Thomas B Schön. A flexible state–space model for learning nonlinear dynamical systems. *Automatica*, 80:189–199, 2017.
- [34] Michalis Titsias. Variational learning of inducing variables in sparse gaussian processes. In *Artificial Intelligence and Statistics*, pages 567–574, 2009.
- [35] Marco Todescato, Andrea Carron, Ruggero Carli, Gianluigi Pillonetto, and Luca Schenato. Efficient spatio-temporal gaussian regression via kalman filtering. *arXiv preprint arXiv:1705.01485*, 2017.
- [36] Grace Wahba, Xiwu Lin, Fangyu Gao, Dong Xi-ang, Ronald Klein, and Barbara Klein. The bias-variance tradeoff and the randomized gacv. In *Advances in Neural Information Processing Systems*, pages 620–626, 1999.
- [37] M. A. Álvarez, D. Luengo, and N. D. Lawrence. Linear latent force models using gaussian processes. *IEEE Transactions on Pattern Analysis and Machine Intelligence*, 35(11):2693–2705, Nov 2013.

A Useful properties

Inversion Lemma

Given invertible matrices $A \in \mathbb{R}^{B \times B}$, $C \in \mathbb{R}^{M \times M}$ and matrices $U \in \mathbb{R}^{B \times M}$, $V \in \mathbb{R}^{M \times B}$, it holds

$$(A + UCV)^{-1} = A^{-1} - A^{-1}U(C^{-1} + VA^{-1}U)^{-1}VA^{-1}. \quad (38)$$

Determinant Lemma

Given invertible matrices $A \in \mathbb{R}^{B \times B}$, $C \in \mathbb{R}^{M \times M}$ and matrices $U \in \mathbb{R}^{B \times M}$, $V \in \mathbb{R}^{M \times B}$, it holds

$$|A + UCV| = |C^{-1} + VA^{-1}U| |C| |A|. \quad (39)$$

Linear Gaussian Systems

Suppose the two Gaussian densities $p(\mathbf{u}) = \mathcal{N}(\mathbf{u}|\boldsymbol{\mu}_0, \boldsymbol{\Sigma}_0)$ and $p(\mathbf{y}|\mathbf{u}) = \mathcal{N}(\mathbf{y}|\mathbf{H}\mathbf{u}, \mathbf{V})$, where $\mathbf{H} \in \mathbb{R}^{N \times M}$ and $\mathbf{V} \in \mathbb{R}^{N \times N}$. Then we can compute

$$p(\mathbf{y}) = \int p(\mathbf{y}|\mathbf{u}) p(\mathbf{u}) d\mathbf{u} \quad (40)$$

$$= \mathcal{N}(\mathbf{y}|\mathbf{H}\boldsymbol{\mu}_0, \mathbf{V} + \mathbf{H}\boldsymbol{\Sigma}_0\mathbf{H}^T);$$

$$p(\mathbf{u}|\mathbf{y}) = \mathcal{N}(\mathbf{u}|\boldsymbol{\Sigma}(\mathbf{H}^T\mathbf{V}^{-1}\mathbf{y} + \boldsymbol{\Sigma}_0^{-1}\boldsymbol{\mu}_0), \boldsymbol{\Sigma}) \quad (41)$$

where $\boldsymbol{\Sigma} = (\boldsymbol{\Sigma}_0 + \mathbf{H}^T\mathbf{V}^{-1}\mathbf{H})^{-1}$.

B Overview of Sparse Inducing point models

DIC

Early attempts to sparse GP regression are based on the

Subset of Regressors or Deterministic Inducing Conditional (SoR/DIC) approximation due to [30], [36] and [31]. The sparse GP predictive distribution $p(f_*|\mathbf{y}) = \mathcal{N}(f_*|\boldsymbol{\mu}_*, \boldsymbol{\Sigma}_*)$ is given by

$$\begin{aligned}\boldsymbol{\mu}_* &= \mathbf{Q}_{*X} (\mathbf{Q}_{XX} + \sigma_n^2 \mathbb{I})^{-1} \mathbf{y} \\ \boldsymbol{\Sigma}_* &= \mathbf{K}_{**} - \mathbf{Q}_{*X} (\mathbf{Q}_{XX} + \sigma_n^2 \mathbb{I})^{-1} \mathbf{Q}_{X*}\end{aligned}\quad (42)$$

and the parameters can be learnt by maximizing the log marginal likelihood

$$\log p(\mathbf{y}|\boldsymbol{\Theta}) = \log \mathcal{N}(\mathbf{y}|\mathbf{0}, \mathbf{Q}_{XX} + \sigma_n^2 \mathbb{I}). \quad (43)$$

However, these methods produce overconfident predictions when leaving the training data.

DIC

In order to produce sensible uncertainty estimates, the *Deterministic Training Conditional* (DTC) approximation has been introduced by [8],[29]. The predictive distribution for this model can be written as

$$\begin{aligned}\boldsymbol{\mu}_* &= \mathbf{Q}_{*X} (\mathbf{Q}_{XX} + \sigma_n^2 \mathbb{I})^{-1} \mathbf{y}, \\ \boldsymbol{\Sigma}_* &= \mathbf{K}_{**} - \mathbf{Q}_{*X} (\mathbf{Q}_{XX} + \sigma_n^2 \mathbb{I})^{-1} \mathbf{Q}_{X*},\end{aligned}\quad (44)$$

where only the first term \mathbf{Q}_{**} in the predictive variance of DIC is replaced with the exact \mathbf{K}_{**} . However, this has a huge effect, namely that outside of the training data the uncertainty can fall back to the prior uncertainty. The marginal likelihood is the same as for DIC.

FITC

A more sophisticated likelihood approximation constitute the *Fully Independent Training Conditional* (FITC) [32] approximation, where the predictive distribution $p(f_*|\mathbf{y}) = \mathcal{N}(f_*|\boldsymbol{\mu}_*, \boldsymbol{\Sigma}_*)$ is given by

$$\begin{aligned}\boldsymbol{\mu}_* &= \mathbf{Q}_{*X} (\overline{\mathbf{K}}_{XX} + \sigma_n^2 \mathbb{I})^{-1} \mathbf{y}, \\ \boldsymbol{\Sigma}_* &= \mathbf{K}_{**} - \mathbf{Q}_{*X} (\overline{\mathbf{K}}_{XX} + \sigma_n^2 \mathbb{I})^{-1} \mathbf{Q}_{X*}.\end{aligned}\quad (45)$$

Compared to DTC, the richer covariance $\mathbf{Q}_{XX} + \text{Diag}[\mathbf{D}_X]$ corrects on the diagonal the approximated with the exact entries. In this model, the parameters $\boldsymbol{\Theta}$ can be learnt by maximizing the log marginal likelihood

$$\log p(\mathbf{y}|\boldsymbol{\Theta}) = \log \mathcal{N}(\mathbf{y}|\mathbf{0}, \overline{\mathbf{K}}_{XX} + \sigma_n^2 \mathbb{I}) \quad (46)$$

of the sparse model. Two generalizations of this model are proposed by [26] (FIC, PITC). The issue with FITC is that optimizing (46) might lead to overfitting and the predictions with (45) are not necessarily close to full GP (1).

VFE

In order to explicitly link the approximating process to full GP, [34] instead proposed to maximize a variational lower bound to the true marginal log likelihood, obtaining the *Variational Free Energy* (VFE) or the *collapsed lower bound*

$$\mathcal{L}_1(\boldsymbol{\Theta}) = \log \mathcal{N}(\mathbf{y}|\mathbf{0}, \mathbf{Q}_{XX} + \sigma_n^2 \mathbb{I}) - \frac{\text{Tr}[\mathbf{D}_X]}{2\sigma_n^2}, \quad (47)$$

where the variational distribution over the inducing points is optimally eliminated and analytically available. The novelty of this bound is that the rightmost term in (47) acts as a regularizer that prevents overfitting and has the effect that the sparse GP predictive distribution in (44) converges rigorously to the exact GP predictive distribution (1) for increasing number of inducing points when optimizing $\boldsymbol{\Theta}$ with (47).

PEP

Recently, [5] presented a sparse inducing point model based on the minimization of an α -divergence which can also be seen as *Power Expectation Propagation* (PEP). For this model, the predictive distribution $p(f_*|\mathbf{y}) = \mathcal{N}(f_*|\boldsymbol{\mu}_*, \boldsymbol{\Sigma}_*)$ is given by

$$\begin{aligned}\boldsymbol{\mu}_* &= \mathbf{Q}_{*X} (\overline{\mathbf{K}}_{XX} + \sigma_n^2 \mathbb{I})^{-1} \mathbf{y}, \\ \boldsymbol{\Sigma}_* &= \mathbf{K}_{**} - \mathbf{Q}_{*X} (\overline{\mathbf{K}}_{XX} + \sigma_n^2 \mathbb{I})^{-1} \mathbf{Q}_{X*},\end{aligned}\quad (48)$$

where $\overline{\mathbf{K}}_{XX} = \mathbf{Q}_{XX} + \alpha \text{Diag}[\mathbf{D}_X]$ and the lower bound to the marginal likelihood is

$$\log \mathcal{N}(\mathbf{y}|\mathbf{0}, \overline{\mathbf{K}}_{XX} + \sigma_n^2 \mathbb{I}) - \frac{1-\alpha}{2\alpha} \sum_{i=1}^N \log \left(1 + \frac{\alpha}{\sigma_n^2} [\mathbf{D}_X]_{ii} \right). \quad (49)$$

This model unifies several previous sparse GP inference approaches including FITC ($\alpha = 1$) and VFE ($\alpha \rightarrow 0$).

C Details for Recursive Gradient Propagation

We show here a detailed computation for recursive gradient propagation from Section 4.1 for the PEP model. For other models, a_k and $\overline{\mathbf{V}}$ from the Table 2 could be used correspondingly. We will use the following notation:

$$\text{diag}[\mathbf{A}] = \mathbf{d}, d_i = a_{ii}$$

$$\begin{aligned}
\text{Diag}[d] &= \mathbf{A}, a_{ii} = d_i, a_{ij} = 0 \\
\mathbf{A} \odot \mathbf{B} &= \mathbf{C}, c_{ij} = a_{ij}b_{ij} \\
\mathbf{A} \div \mathbf{B} &= \mathbf{C}, c_{ij} = \frac{a_{ij}}{b_{ij}} \\
\mathbf{A}^{\odot 2} &= \mathbf{C}, c_{ij} = a_{ij}^2 \\
\dot{\mathbf{A}} &= \frac{\partial \mathbf{A}(\theta)}{\partial \theta}, \forall \theta \in \Theta \\
\text{sum}[\mathbf{A}] &= \sum_{i,j} a_{ij} \\
1_{[z]} &= 1 \text{ if } z = \text{true}, 0 \text{ otherwise}
\end{aligned}$$

Initialization

$$\begin{aligned}
\eta_0 &= \mathbf{0}; & \dot{\eta}_0 &= \mathbf{0}; \\
\Lambda_0 &= \mathbf{K}_{RR}^{-1}; & \dot{\Lambda}_0 &= -\mathbf{K}_{RR}^{-1} \dot{\mathbf{K}}_{RR} \mathbf{K}_{RR}^{-1}; \\
\psi_0 &= -\frac{N}{2} \log 2\pi; & \dot{\psi}_0 &= \mathbf{0}; \\
\Sigma_0 &= \mathbf{K}_{RR}; & \log \text{Det}_0 &= \log |\Lambda_0|;
\end{aligned}$$

Natural Mean and Precision Updates

$$\begin{aligned}
\mathbf{H}_k &= \mathbf{K}_{X_k R} \mathbf{K}_{RR}^{-1}; \\
\mathbf{d}_k &= \text{diag}[\mathbf{K}_{X_k X_k} - \mathbf{K}_{X_k R} \mathbf{K}_{RR}^{-1} \mathbf{K}_{R X_k}]; \\
\mathbf{v}_k &= \alpha \mathbf{d}_k + \sigma_n^2 \mathbb{1}; \\
\mathbf{V}_k^{-1} &= \text{Diag}[\mathbb{1} \div \mathbf{v}_k]; \\
a_k &= \frac{1-\alpha}{\alpha} \left(\sum_{i=1}^B \log([\mathbf{v}_k]_i) - B \log \sigma_n^2 \right); \\
\mathbf{r}_k &= \mathbf{y}_k - \mathbf{H}_k \Sigma_{k-1} \eta_{k-1}; \\
\eta_k &= \eta_{k-1} + \mathbf{H}_k^T \mathbf{V}_k^{-1} \mathbf{y}_k; \\
\Lambda_k &= \Lambda_{k-1} + \mathbf{H}_k^T \mathbf{V}_k^{-1} \mathbf{H}_k; \\
\Sigma_k, \log |\Lambda_k| &= \Lambda_k^{-1}, \log |\Lambda_k|; \\
\mathbf{S}_k^{-1} &= \mathbf{V}_k^{-1} - \mathbf{V}_k^{-1} \mathbf{H}_k \Sigma_k \mathbf{H}_k^T \mathbf{V}_k^{-1}; \\
\psi_k &= \psi_{k-1} - \frac{1}{2} (\log |\Lambda_k| - \log |\Lambda_{k-1}| \\
&\quad - \log |\mathbf{V}_k^{-1}| + \mathbf{r}_k^T \mathbf{S}_k^{-1} \mathbf{r}_k + a_k)
\end{aligned}$$

Intermediate Derivatives

$$\begin{aligned}
\dot{\mathbf{L}}_{d\mathbf{H}_k} &= 2(\mathbf{V}_k^{-1} \mathbf{H}_k \Sigma_k - \mathbf{S}_k^{-1} \mathbf{r}_k (\Sigma_{k-1} \eta_{k-1} \\
&\quad + \Sigma_k \mathbf{H}_k^T \mathbf{V}_k^{-1} \mathbf{r}_k)^T)
\end{aligned}$$

$$\begin{aligned}
\dot{\mathbf{L}}_{d\mathbf{v}_k} &= - \left(\text{diag}[\mathbf{H}_k \Sigma_k \mathbf{H}_k^T] - \frac{1}{\alpha} \mathbf{v}_k \right. \\
&\quad \left. + (\mathbf{r}_k - \mathbf{H}_k \Sigma_k \mathbf{H}_k^T \mathbf{V}_k^{-1} \mathbf{r}_k)^{\odot 2} \right) \div \mathbf{v}_k^{\odot 2} \\
\dot{\mathbf{L}}_{d\mathbf{K}_{X_k R}} &= \dot{\mathbf{L}}_{d\mathbf{H}_k} \mathbf{K}_{RR}^{-1} - 2\alpha \text{Diag}[\dot{\mathbf{L}}_{d\mathbf{v}_k}] \mathbf{H}_k \\
\dot{\mathbf{L}}_{d\mathbf{K}_{RR}} &= -\mathbf{H}_k^T (\dot{\mathbf{L}}_{d\mathbf{H}_k} \mathbf{K}_{RR}^{-1} - \alpha \text{Diag}[\dot{\mathbf{L}}_{d\mathbf{v}_k}] \mathbf{H}_k) \\
\dot{\mathbf{L}}_{d\mathbf{k}_{X_k X_k}} &= \alpha \dot{\mathbf{L}}_{d\mathbf{v}_k} \\
\dot{\mathbf{L}}_{d\Lambda_k} &= \Sigma_k - \Sigma_{k-1} + 2\Sigma_{k-1} \mathbf{H}_k^T \mathbf{S}_k^{-1} \mathbf{r}_k \eta_{k-1}^T \Sigma_{k-1} \\
&\quad + \Sigma_k \mathbf{H}_k^T \mathbf{V}_k^{-1} \mathbf{r}_k \mathbf{r}_k^T \mathbf{V}_k^{-1} \mathbf{H}_k \Sigma_k \\
\dot{\mathbf{L}}_{d\eta_k} &= -2\Sigma_{k-1} \mathbf{H}_k^T \mathbf{S}_k^{-1} \mathbf{r}_k \\
\dot{\mathbf{L}}_{d_{d_n}} &= 2\sigma_n^2 \text{sum}[\dot{\mathbf{L}}_{d\mathbf{v}_k}] - 2B \frac{1-\alpha}{\alpha}
\end{aligned}$$

Derivative Updates

Loop over $\theta \in \Theta$:

$$\begin{aligned}
\dot{\psi}_k &= \dot{\psi}_{k-1} - \frac{1}{2} (\text{sum}[\dot{\mathbf{L}}_{d\eta_k} \odot \dot{\eta}_{k-1}] \\
&\quad + \text{sum}[\dot{\mathbf{L}}_{d\Lambda_k} \odot \dot{\Lambda}_{k-1}] + \text{sum}[\dot{\mathbf{L}}_{d\mathbf{K}_{RR}} \odot \dot{\mathbf{K}}_{RR}] \\
&\quad + \text{sum}[\dot{\mathbf{L}}_{d\mathbf{K}_{X_k R}} \odot \dot{\mathbf{K}}_{X_k R}] \\
&\quad + \text{sum}[\dot{\mathbf{L}}_{d\mathbf{k}_{X_k X_k}} \odot \dot{\mathbf{k}}_{X_k X_k}] + 1_{[\Theta_k = \sigma_n]} \dot{\mathbf{L}}_{d_{d_n}}) \\
\dot{\mathbf{H}}_k &= \dot{\mathbf{K}}_{X_k R} \mathbf{K}_{RR}^{-1} - \mathbf{K}_{X_k R} \mathbf{K}_{RR}^{-1} \dot{\mathbf{K}}_{RR} \mathbf{K}_{RR}^{-1}; \\
\dot{\mathbf{d}}_k &= \text{diag}[\dot{\mathbf{K}}_{X_k X_k} - \dot{\mathbf{K}}_{X_k R} \mathbf{K}_{RR}^{-1} \mathbf{K}_{R X_k} \\
&\quad + \mathbf{K}_{X_k R} \mathbf{K}_{RR}^{-1} \dot{\mathbf{K}}_{RR} \mathbf{K}_{RR}^{-1} \mathbf{K}_{R X_k} \\
&\quad - \mathbf{K}_{X_k R} \mathbf{K}_{RR}^{-1} \dot{\mathbf{K}}_{R X_k}]; \\
\dot{\mathbf{V}}_k^{-1} &= -1_{[\Theta_k \neq \sigma_n]} \alpha \mathbf{V}_k^{-1} \text{Diag}[\dot{\mathbf{d}}_k] \mathbf{V}_k^{-1} \\
&\quad - 1_{[\Theta_k = \sigma_n]} 2\sigma_n^2 \dot{\mathbf{V}}_k^{-1} \mathbf{V}_k^{-1}; \\
\dot{\eta}_k &= \dot{\eta}_{k-1} + \dot{\mathbf{H}}_k^T \mathbf{V}_k^{-1} \mathbf{y}_k + \mathbf{H}_k^T \dot{\mathbf{V}}_k^{-1} \mathbf{y}_k; \\
\dot{\Lambda}_k &= \dot{\Lambda}_{k-1} + \dot{\mathbf{H}}_k^T \mathbf{V}_k^{-1} \mathbf{H}_k \\
&\quad + \mathbf{H}_k^T \dot{\mathbf{V}}_k^{-1} \mathbf{H}_k + \mathbf{H}_k^T \mathbf{V}_k^{-1} \dot{\mathbf{H}}_k
\end{aligned}$$

For the noise σ_n , all kernel derivatives are zero, therefore the calculations simplify significantly.

D Derivation of Recursive Collapsed Bound

We provide more details and a detailed derivation for the recursive collapsed lower bound (28) for the VFE model from Section 4.1. Instead of lower bounding directly the batch marginal likelihood as done by Titsias [34] in the batch case,

our approach relies on the recursive factorization of the joint marginal log-likelihood $\log p(\mathbf{y}|\Theta) = \log \prod_{k=1}^K p(\mathbf{y}_k|\mathbf{y}_{1:k-1}, \Theta) = \sum_{k=1}^K \log p(\mathbf{y}_k|\mathbf{y}_{1:k-1}, \Theta)$. Exploiting the properties induced by the sparse augmented inducing point model yields $\log p(\mathbf{y}|\Theta) = \sum_{k=1}^K \log \int p(\mathbf{y}_k|\mathbf{f}_k, \Theta) p(\mathbf{f}_k|\mathbf{u}, \Theta) p(\mathbf{u}|\mathbf{y}_{1:k-1}, \Theta) d\mathbf{f}_k d\mathbf{u}$. Let us now introduce the variational distributions $q_k(\mathbf{f}_k, \mathbf{u}) = p(\mathbf{f}_k|\mathbf{u}, \Theta) q_k(\mathbf{u}) \approx p(\mathbf{f}_k, \mathbf{u}|\mathbf{y}_{1:k}, \Theta)$, then by applying Jensen's inequality to each individual term in the true marginal log-likelihood, we obtain the following lower bound

$$\log p(\mathbf{y}|\Theta) \geq \sum_{k=1}^K \int p(\mathbf{f}_k|\mathbf{u}, \Theta) q_k(\mathbf{u}) \dots \dots \log \frac{p(\mathbf{y}_k|\mathbf{f}_k, \Theta) p(\mathbf{f}_k|\mathbf{u}, \Theta) p(\mathbf{u}|\mathbf{y}_{1:k-1}, \Theta)}{p(\mathbf{f}_k|\mathbf{u}, \Theta) q_k(\mathbf{u})} d\mathbf{f}_k d\mathbf{u}.$$

The quantity $p(\mathbf{u}|\mathbf{y}_{1:k-1}, \Theta)$ is unknown, however, we can replace it with $q_{k-1}(\mathbf{u})$ leading to $\mathcal{L}(q_1, \dots, q_K, \Theta)$

$$\sum_{k=1}^K \int p(\mathbf{f}_k|\mathbf{u}, \Theta) q_k(\mathbf{u}) \log \frac{p(\mathbf{y}_k|\mathbf{f}_k, \Theta) q_{k-1}(\mathbf{u})}{q_k(\mathbf{u})} d\mathbf{f}_k d\mathbf{u}. \quad (50)$$

Maximizing this lower bound recursively with respect to the distributions $q_k(\mathbf{u})$ leads to a sequence of optimal variational distributions $q_k^*(\mathbf{u})$ for the inducing outputs

$$\mathcal{N}\left(\mathbf{u}|\Sigma_k \left\{ \frac{1}{\sigma_n^2} \mathbf{H}_k^T \mathbf{y}_k + \Sigma_{k-1}^{-1} \boldsymbol{\mu}_{k-1} \right\}, \Sigma_k\right), \quad (51)$$

where $\Sigma_k = \left(\Sigma_{k-1}^{-1} + \frac{1}{\sigma_n^2} \mathbf{H}_k^T \mathbf{H}_k \right)^{-1}$ and $\mathbf{H}_k = \mathbf{K}_{\mathbf{X}_k \mathbf{R}} \mathbf{K}_{\mathbf{R} \mathbf{R}}^{-1}$. Plugging $q_k^*(\mathbf{u})$ back into (50) yields the *recursive collapsed bound*

$$\mathcal{L}_{REC}(\Theta) = \sum_{k=1}^K \left[\log \mathcal{N}(\mathbf{y}_k | \mathbf{H}_k \boldsymbol{\mu}_{k-1}, \dots \dots \mathbf{H}_k \Sigma_{k-1} \mathbf{H}_k^T + \sigma_n^2 \mathbb{I}) - \frac{\text{Tr}[\mathbf{D}_{\mathbf{X}_k \mathbf{X}_k}]}{2\sigma_n^2} \right]. \quad (52)$$

This recursive bound $\mathcal{L}_{REC}(\Theta)$ is equivalent to the batch collapsed bound $\mathcal{L}_{VFE}(\Theta)$ in (5) and it holds $\mathcal{L}_{SVGP}(\boldsymbol{\mu}, \boldsymbol{\Sigma}, \Theta) \leq \mathcal{L}_{REC}(\Theta)$ with equality when inserting the optimal sequence of the variational posterior. We can observe that the variational posterior update in (51) has the same form as the recursive update equations in (15). Similarly, the recursive collapsed lower bound in (52) is equal to the lower bound in (28).

A detailed derivation is provided below. We closely follow the proof in [34] for proving the recursive collapsed bound (52) as well as the sequence of optimal distributions (51). We assume mini-batches of size B , that is, we have training data $\mathcal{D} = \{\mathbf{y}_k, \mathbf{X}_k\}_{k=1}^K$ and the corresponding latent function values $\{\mathbf{f}_k\}_{k=1}^K$. We briefly recap the involved quantities and introduce abbreviations:

$$\begin{aligned} p(\mathbf{y}_k|\mathbf{f}_k, \Theta) &= \mathcal{N}(\mathbf{y}_k|\mathbf{f}_k, \sigma_n^2 \mathbb{I}); \\ p(\mathbf{f}_k|\mathbf{u}, \Theta) &= \mathcal{N}(\mathbf{f}_k|\mathbf{H}_k \mathbf{u}, \mathbf{K}_{\mathbf{X}_k \mathbf{X}_k} - \mathbf{Q}_{\mathbf{X}_k \mathbf{X}_k}); \\ p(\mathbf{u}|\Theta) &= \mathcal{N}(\mathbf{u}|\mathbf{0}, \mathbf{K}_{\mathbf{R} \mathbf{R}}) = q_0(\mathbf{u}); \\ q_{k-1}(\mathbf{u}) &= \mathcal{N}(\mathbf{u}|\boldsymbol{\mu}_{k-1}, \boldsymbol{\Sigma}_{k-1}) \approx p(\mathbf{u}|\mathbf{y}_{1:k-1}, \Theta) \\ \mathbf{H}_k &= \mathbf{K}_{\mathbf{X}_k \mathbf{R}} \mathbf{K}_{\mathbf{R} \mathbf{R}}^{-1}; \\ \mathbf{Q}_{\mathbf{X}_k \mathbf{X}_k} &= \mathbf{K}_{\mathbf{X}_k \mathbf{R}} \mathbf{K}_{\mathbf{R} \mathbf{R}}^{-1} \mathbf{K}_{\mathbf{R} \mathbf{X}_k}. \end{aligned}$$

Starting from (50), we have the bound

$$\sum_{k=1}^K \int p(\mathbf{f}_k|\mathbf{u}, \Theta) q_k(\mathbf{u}) \log \frac{p(\mathbf{y}_k|\mathbf{f}_k, \Theta) q_{k-1}(\mathbf{u})}{q_k(\mathbf{u})} d\mathbf{f}_k d\mathbf{u}$$

which can be rearranged to

$$\sum_{k=1}^K \int q_k(\mathbf{u}) \left\{ \log G(\mathbf{u}, \mathbf{y}_k) + \log \frac{q_{k-1}(\mathbf{u})}{q_k(\mathbf{u})} \right\} d\mathbf{u},$$

where $\log G(\mathbf{u}, \mathbf{y}_k) = \int p(\mathbf{f}_k|\mathbf{u}, \Theta) \log p(\mathbf{y}_k|\mathbf{f}_k, \Theta) d\mathbf{f}_k$. The integral involving \mathbf{f}_k is computed as follows

$$\log G(\mathbf{u}, \mathbf{y}_k) = \int p(\mathbf{f}_k|\mathbf{u}, \Theta) \log p(\mathbf{y}_k|\mathbf{f}_k, \Theta) d\mathbf{f}_k$$

which equals

$$\begin{aligned} &= \mathbb{E}_{\mathbf{f}_k|\mathbf{u}} \left[-\frac{B}{2} \log(2\pi\sigma_n^2) - \frac{1}{2} [\mathbf{y}_k - \mathbf{f}_k]^T \frac{1}{\sigma_n^2} [\mathbf{y}_k - \mathbf{f}_k] \right] \\ &= -\frac{B}{2} \log(2\pi\sigma_n^2) - \frac{1}{2\sigma_n^2} (\mathbf{y}_k^T \mathbf{y}_k + \mathbb{E}_{\mathbf{f}_k|\mathbf{u}} [\mathbf{f}_k^T \mathbf{f}_k - 2\mathbf{y}_k^T \mathbf{f}_k]). \end{aligned}$$

Using $\mathbb{E}[\mathbf{x}^T \mathbf{A} \mathbf{x}] = \text{Tr}[\mathbf{A} \boldsymbol{\Sigma}] + \boldsymbol{\mu}^T \mathbf{A} \boldsymbol{\mu}$ with $p(\mathbf{x}) = \mathcal{N}(\mathbf{x}|\boldsymbol{\mu}, \boldsymbol{\Sigma})$ yields

$$\begin{aligned} \log G(\mathbf{u}, \mathbf{y}_k) &= -\frac{K}{2} \log(2\pi\sigma_n^2) - \frac{1}{2\sigma_n^2} (\mathbf{y}_k^T \mathbf{y}_k \\ &+ \text{Tr}[\mathbf{K}_{\mathbf{X}_k \mathbf{X}_k} - \mathbf{Q}_{\mathbf{X}_k \mathbf{X}_k}] + \mathbf{u}^T \mathbf{H}_k^T \mathbf{H}_k \mathbf{u} - 2\mathbf{y}_k^T \mathbf{H}_k \mathbf{u}) \\ &= \log [\mathcal{N}(\mathbf{y}_k|\mathbf{H}_k \mathbf{u}, \sigma_n^2 \mathbb{I})] - \frac{1}{2\sigma_n^2} \text{Tr}[\mathbf{K}_{\mathbf{X}_k \mathbf{X}_k} - \mathbf{Q}_{\mathbf{X}_k \mathbf{X}_k}]. \end{aligned}$$

Substitute this expression back, the lower bound becomes

$$\sum_{k=1}^K \left[\int q_k(\mathbf{u}) \log \frac{\mathcal{N}(\mathbf{y}_k | \mathbf{H}_k \mathbf{u}, \sigma_n^2 \mathbb{I}) q_{k-1}(\mathbf{u})}{q_k(\mathbf{u})} d\mathbf{u} - \frac{1}{2\sigma_n^2} \text{Tr} [\mathbf{K}_{\mathbf{X}_k \mathbf{X}_k} - \mathbf{Q}_{\mathbf{X}_k \mathbf{X}_k}] \right].$$

We can now maximize this bound with respect to $q_k(\mathbf{u})$. The usual way of doing this is to take the functional derivative with respect to q_b and set it to zero. However, since q_b was not constrained to belong to any restricted family of distributions, a faster and by far simpler way to compute the optimal bound is by reversing the Jensen's inequality leading to

$$\begin{aligned} \mathcal{L}_{REC}(\Theta) &= \sum_{k=1}^K \left[\log \int \mathcal{N}(\mathbf{y}_k | \mathbf{H}_k \mathbf{u}, \sigma_n^2 \mathbb{I}) q_{k-1}(\mathbf{u}) d\mathbf{u} - \frac{1}{2\sigma_n^2} \text{Tr} [\mathbf{K}_{\mathbf{X}_k \mathbf{X}_k} - \mathbf{Q}_{\mathbf{X}_k \mathbf{X}_k}] \right] \\ &= \sum_{k=1}^K \left[\log \mathcal{N}(\mathbf{y}_k | \mathbf{H}_k \boldsymbol{\mu}_{k-1}, \mathbf{H}_k \boldsymbol{\Sigma}_{k-1} \mathbf{H}_k^T + \sigma_n^2 \mathbb{I}) - \frac{1}{2\sigma_n^2} \text{Tr} [\mathbf{K}_{\mathbf{X}_k \mathbf{X}_k} - \mathbf{Q}_{\mathbf{X}_k \mathbf{X}_k}] \right] \end{aligned}$$

where we used (40) in the last step. This result is equal to Equation (28). The optimal distribution q_k^* that gives rise to this bound is proportional to

$$\begin{aligned} &\mathcal{N}(\mathbf{y}_k | \mathbf{H}_k \mathbf{u}, \sigma_n^2 \mathbb{I}) q_{k-1}(\mathbf{u}) \\ &= \mathcal{N}(\mathbf{y}_k | \mathbf{H}_k \mathbf{u}, \sigma_n^2 \mathbb{I}) \mathcal{N}(\mathbf{u} | \boldsymbol{\mu}_{k-1}, \boldsymbol{\Sigma}_{k-1}) \end{aligned}$$

and can be analytically computed leading to

$$q_k^*(\mathbf{u}) = \mathcal{N}\left(\mathbf{u} \mid \frac{1}{\sigma_n^2} \boldsymbol{\Sigma}_k \mathbf{H}_k^T \mathbf{y}_k + \boldsymbol{\Sigma}_{k-1}^{-1} \boldsymbol{\mu}_{k-1}, \boldsymbol{\Sigma}_k\right)$$

where $\boldsymbol{\Sigma}_k = \left(\boldsymbol{\Sigma}_{k-1}^{-1} + \frac{1}{\sigma_n^2} \mathbf{H}_k^T \mathbf{H}_k\right)^{-1}$. This matches the result in Equation (15) and (16) and completes the proof.